STABILITY ANALYSIS OF A THREE-DIMENSIONAL QUADRUPED TROTTING ROBOT WITH PASSIVE COMPLIANT LEGS

by

Mohammad Reza Yazdi Samadi

A thesis submitted to the faculty of
The University of Utah
in partial fulfillment of the requirements for the degree of

Master of Science

Department of Mechanical Engineering

The University of Utah

December 2012

The University of Utah Graduate School

STATEMENT OF THESIS APPROVAL

The thesis of **Mohammad Reza Yazdi Samadi**

has been approved by the following supervisory committee members:

Sanford Meek	, Chair	**10.25.2012** Date Approved
Stacy Morris Bamberg	, Member	**10.25.2012** Date Approved
Mark Minor	, Member	**10.25.2012** Date Approved

and by **Timothy Ameel** , Chair of

the Department of **Mechanical Engineering**

and by Charles A. Wight, Dean of The Graduate School.

ABSTRACT

This research studies the passive dynamics of an under-actuated trotting quadruped. The goal of this project is to perform three-dimensional (3D) dynamic simulations of a trotting quadruped robot to find proper leg configurations and stiffness range, in order to achieve stable trotting gait. First, a 3D simulation framework that includes all the six degrees of freedom of the body is introduced. Directionally compliant legs together with different leg configurations are employed to achieve passive stability. Compliant legs passively support the body during stance phase and during flight phase a motor is used to retract the legs. Leg configurations in the robot's sagittal and frontal plane are introduced. Numerical experiments are conducted to search the design space of the leg, focusing on increasing the passive stability of the robot. Increased stability is defined as decreased pitching, rolling, and yawing motion of the robot. The results indicate that optimized leg parameters can guarantee passive stable trotting with reduced roll, pitch, and yaw. Studies suggest that a quadruped robot with compliant legs is dynamically stable while trotting. Results indicate that the robot based on a biological model (i.e., caudal inclination of humeri and cranial inclination of femora) has the best performance. Stiff springs at hips and shoulders, soft spring at knees and elbows, and stiff springs at ankles and wrists are recommended. The results of this project provide a conceptual framework for understanding the movements of a trotting quadruped.

To my mother and father

TABLE OF CONTENTS

LIST OF TABLES

LIST OF FIGURES

ACKNOWLEDGEMENTS

This research project would not have been possible without the support of many people. The author wishes to express his gratitude to his supervisor, Dr. Sanford Meek, who was abundantly helpful and offered invaluable assistance, support and guidance. Deepest gratitude are also due to the members of the supervisory committee, Dr. Mark Minor and Dr. Stacy Bamberg, without whose knowledge and assistance this study would not have been successful.

The author wishes to express his love and gratitude to his beloved family; for their understanding and endless support, through the duration of his studies.

CHAPTER 1

INTRODUCTION

Research in the area of legged robots is a very attractive topic for scientists and engineers. The reason is that these robots are capable of navigating through rough terrain, and they can be used to perform various tasks such as: search and rescue, exploration, military purposes, transportation, etc.

Legged Robots

Legged robots are able to navigate through irregular terrain by actuating each leg separately. However, legged robots are fundamentally more complex in structure and control than the wheeled robots [1, 7, 9, 15]. In spite of various stability and attitude-control problems, quadrupeds have shown great mobility on different surfaces at different speeds [20, 22, 26-28]. Most of the research in this area is categorized into two groups: machines utilizing feed-back or feed-forward control. Research in the area of quadrupeds that employ feed-forward control is primarily focused on how to promote dynamical stability of a running quadruped [1, 5-9, 31].

Increasing the speed and robustness of such robots would result in more efficiency. This project is based on the hypothesis that through proper design of leg compliance and configuration, stability could be improved passively, which would in turn

increase the robustness of the robot. In order to achieve stability in higher locomotion speeds, a trotting model was chosen for this study. Trotting is statically unstable, because a quadruped while trotting has only two feet on the ground at each instance in time. The same feature makes trotting energy efficient and suitable for travel. This high speed gait is widely seen in mammalian quadrupeds capable of walking and running [22, 28].

The goal of this study is to utilize passive compliant legs in a trotting quadruped. Additionally, in order to accomplish a better understanding of the nature of quadruped locomotion a conceptual framework has been provided through investigating the effect of different leg parameters such as stiffness and damping, leg postures, stride length, etc. on the passive stability of a quadruped trotting model at different speeds. Researchers have shown that directionally compliant joints greatly assist the pitch stability of a robot [11-16, 25]. However, previous research, with the exception of BigDog [46-48], was merely confined to 2D models or low speed gaits. Unfortunately, Boston Dynamics' BigDog is a defence robot and the information on it is confidential and it's of no use to researchers. It is desired to provide a 3D framework to verify previous results and to examine the roll and yaw behavior of a quadruped while trotting. This would become a powerful utility for future design purposes.

The first step consisted of the design of a simulation model that could be used to analyze the kinematics and kinetics of a multilegged trotting robot in 3D. A computer model was generated using MATLAB/Simulink and the SimMechanics toolbox [17]. This software uses relative coordinate formulation along with numerical integration to solve the equations of motion [18]. Integrating the multibody analysis capabilities of the SimMechanics and powerful programming utilities of MATLAB along with practical

control systems toolboxes would result in a powerful analysis of the quadruped trotting. Addition of different controllers in the future studies would become much easier using Simulink capabilities if the system is already modeled in the SimMechanics. The second phase of this project was use of the models to increase the stability of the trotting quadruped. The simulations that were conducted through the course of this project focused on various leg parameters that are introduced in Chapter 3, as well as several parameters corresponding with robot speed. Steady-state response of the simulations was analyzed in different speeds and to verify previous results in terms of joint springs and limb configuration. Finally, the robot performance is tested under disturbances to gain an understanding of a passive under-actuated robot's tolerance to disturbance. If the robot is capable of rejecting disturbance effects passively, it would be more robust if it is accompanied by feed-back control algorithms. However, the use of a passively stable robot accompanied by feed-back control is not in the scope of this research.

The motion of the robot is not constrained, and the body has all the 6 degrees of freedom (DOF). Furthermore, the legs of the robot will be under-actuated. It has four legs with 4 DOF each, and yet each leg is controlled by only one motor. For the trotting gait, a motor could be used to actuate two diagonal legs, because they have the exact same motion. The motors are controlled by a tabular feed-forward controller. The remaining degrees of freedom such as ankle/wrist, knee/elbow, etc. are supported by joint springs and dampers.

The remainder of this project will proceed as follows. Previous work on the area of quadruped robots, especially the use of directionally compliant legs, is investigated in Chapter 2. Chapter 3 describes in detail the design of the computer model according to

MATLAB/Simulink and SimMechanics toolbox. Simulation results (i.e.,, steady-state and disturbance responses) along with some discussions are presented in Chapter 4. Finally, the conclusions and suggestions are presented in Chapter 5.

CHAPTER 2

BACKGROUND

There are two main reasons for exploring the use of legs for locomotion. One is mobility: there is a need for machines that can travel on irregular terrain. Wheels excel on the prepared surfaces such as rails and roads, but perform poorly where the surface is soft or uneven. Because of these limitations, about half of the earth's landmass is not accessible to existing wheeled or tracked machines, whereas a much greater area can be reached by animals on foot. One reason legs provide better mobility in rough terrain is that they can use isolated footholds that optimize support and traction, whereas a wheel requires a continuous path of support [30]. As a consequence, a legged system can choose among the best footholds in the reachable terrain; a wheel must negotiate the worst terrain. Another advantage of legs is that they provide an active suspension that decouples the path of the body from the paths of the feet. The payload is free to travel smoothly despite pronounced variation in the terrain. A legged system can also step over obstacles. Legged vehicles will need systems that control joint motions, sequence the use of legs, monitor and manipulate balance, generate motions to use known footholds, sense the terrain to find good footholds, and calculate negotiable foothold sequences [30].

The second reason for studying legged locomotion is to gain a better understanding of human and animal locomotion. [30]

Biological Inspiration

Gait

A gait is defined as the periodic pattern of locomotion characterized to a specific range of speed. Some common quadruped gaits are walk, pace, bound, amble, trot, canter, slow gallop, and gallop. Through the course of evolution, each gait has been optimized to minimize energy consumption for a specified speed.

The trot gait is commonly used in legged robot researches [1, 7, 10, 11] and is the focus of this research. The trot is defined by the legs acting together in diagonal pairs. The right front leg is retracted with the left rear leg and the left front leg is retracted with the right rear leg. The two diagonal pairs are half a cycle out of phase, producing an alternate pattern of diagonal foot contact (Fig. 1).

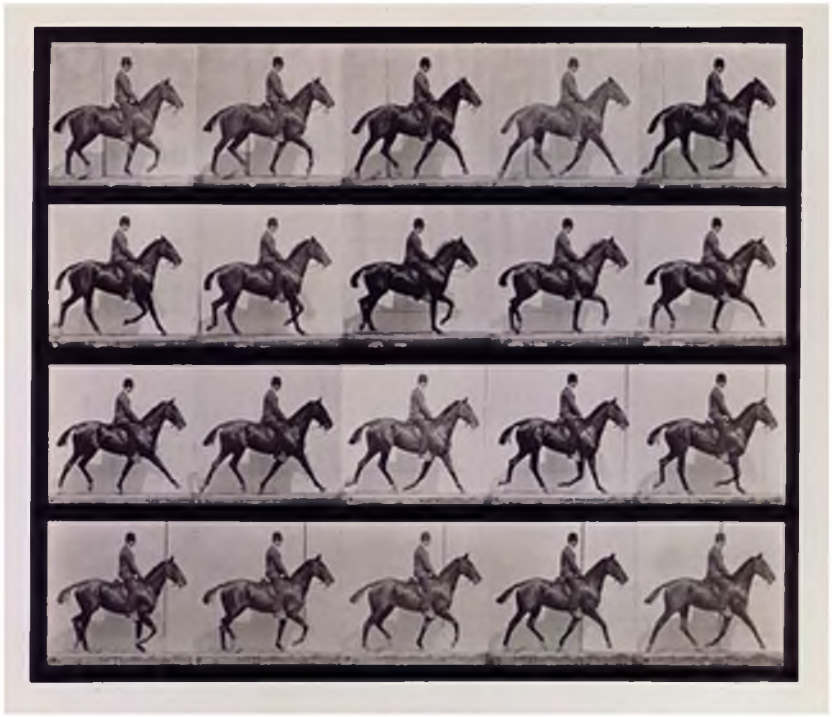

Fig. 1 – The trot. Plate from *Animals in Motion*, United States, 1887 by Eadweard Muybridge, AMNH Library

Froude Number

The change in different gaits occurs at specific speeds. In order to normalize animal speeds across different body sizes so that locomotion of different animals can be compared, the Froude number is introduced. The Froude number is an important parameter in describing animal gaits and is defined as:

$$Froude\ Number = \frac{(speed)^2}{(g)(hip\ or\ shoulder\ height)} \quad (1)$$

in which; g is the gravitational acceleration. It has been shown that animals change gaits at similar Froude numbers [22, 23]. For example, humans generally change from walking to running at the Froude number of approximately 0.5. Transition from walking to trotting in quadruped mammals happens approximately at Froude number of 0.5 and transition to galloping happens approximately at Froude number of 2.5. For additional details on the definition and applications of Froude number on quadruped locomotion, refer to [22, 23].

Previous Work on Quadruped Robots

Beginning in the 1980s and continuing into the 2000s, several researchers developed quadruped robots using active balance controls [1, 4, 5, 6]. However, in 1990 McGeer questioned the active balance paradigm by arguing that legged machines should be naturally stable, not requiring feedback of body posture [2, 3]. After McGeer's work, other researchers suggested that his work on bipeds could be generalized to quadruped machines. Similar to mammalian quadrupeds, quadruped machines can also be

dynamically stable without using feedback control [29]. However, passive walkers only perform on inclined surfaces.

In 1998, Matthew Berkemeier [9] presented a 2-DOF model of quadruped running gaits, including bound and pronk. He used a spring, a damper and position-controlled actuator on each leg. His research revealed that by intelligent choice of different parameter values and utilizing a controller that included energy pumping, attitude control, and virtual legs, stable running could be demonstrated. However, his work was limited to only low speed running gaits.

In attempts to improve robotics stability, Herr and McMahon [7, 8] raised the question of "Do animals remain balanced while trotting by actively controlling body posture throughout ground contact, or are they naturally stable because of an inherently stable body shape?" [7 pp. 567] They discovered that a horse like robot does not have to actively balance to remain upright from running cycle to running cycle. In fact, pitch stabilization could be achieved indirectly by controlling when each foot begins to retract toward the ground and how fast each stance foot moves relative to the model's trunk during ground contact.

Several researchers looked into the compliance of individual joints or to use of compliant prismatic legs [10-15]. Martin Buehler and colleagues at McGill University developed several robots, from monopods to hexapods. SCOUT II-k, a trotting quadruped robot with passive knees, unveiled that it is possible to reach stable trot utilizing passive knees [10]. They achieved stable trotting in experiment, despite the fact that, their simulation results where different from experimental results. Later on, the same robot was tested employing compliant prismatic legs [15]. The most remarkable feature of

SCOUT II was the fact that it used only a single actuator per leg located at the hip/shoulder joint. Although this research was merely limited to bounding gait, it instantiated fundamental design and control principles for a new class of quadrupeds with reduced mechanical complexity and power requirements.

Meek and colleagues at University of Utah [11, 16]; investigated the role of passive, under-actuated directionally-compliant legs. They presented 2D computer models of quadruped machines based on biological quadrupeds. The models were implemented using Raibert's principle of virtual legs [1], in which pairs of legs were controlled to act like one leg. They illustrated means of enhancing the passive stability by intelligently choosing leg postures in the sagittal plane (i.e.,, caudal inclination of humeri and cranial inclination of femora) and different leg spring and damper coefficients. However, they constructed their models in Working Model 2D™, which would constrain the legs and trunk to move only in the sagittal plane. Consequently, the researches were only limited to the pitch behavior of the robot and the effects of the roll and yaw on the passive stability of the quadruped were ignored.

Orin et al. [32, 33] investigated the galloping of a high speed quadruped to find the most energy-efficient, natural, and unconstrained gallop that can be achieved using a simulated quadruped robot with compliant legs. They introduced a new control approach based on heuristic knowledge of the quadruped mechanics and were able to achieve better velocity and height tracking characteristics than a Raibert-based controller. Later on, Orin and colleagues built and tested a goat-sized quadruped robot to further understand the primary biological features necessary for galloping [34]. The features

comprised high-speed actuation, energy storage, online learning control, and high performance attitude sensing.

Researchers at the Italian Institute of Technology (IIT) utilized hydraulic actuations in quadruped legs [36, 38, 39]. Their new versatile hydraulically powered quadruped robot (HyQ) is a quadruped robot that has hybrid actuation: hydraulic and electric. They also introduced semiactive dampers to assist the control of robots powered by compliant actuators [37]. They required control, both on hydraulic level (force/torque control) and whole body level (rigid model based control).

A trotting quadruped cannot employ traditional stability techniques such as zero moment point [49]. Instead, the corrective forces necessary to maintain dynamic stability must be applied during the short stance intervals inherent to high-speed running. Because of this complexity and the large coupled forces required to run, much of the research on the control of quadruped running has focused on planar systems that are not required to simultaneously control attitude in all three dimensions. Palmer and Orin [42-44], at the Ohio State University presented a 3D trot controller to overcome these and other complexities to control a trot. It utilized a hybrid control system using a discrete controller running once per step and a continuous controller during stance that dynamically stabilized a quadruped running at 3.75 m/s (approximately 3 body lengths per second), and turning at 20 deg/s [43]. Such speeds and turning rates were attainable because the force redistribution algorithm implemented during stance corrected the pitch and roll motion without impacting the forward, lateral, vertical, or yaw motion. Later on, by adding a fuzzy controller and a force redistribution algorithm, they were able to

stabilize a quadruped trot at 5.25 m/s, (approximately four body lengths per second), and turning at 30 deg/s [42, 44].

Motivation

The machines described thus far (with the exceptions of Orin's robots and BigDog), although functional in some sense, were only limited to low speed gaits or 2D models. Herr and McMahon's trotting horse model was confined to the sagittal plane motion. Buehler's machines, although compelling from the energy efficiency perspective, are limited to low speed gaits (i.e., bounding). Previous research by Meek et al. [16]; verified that through proper design of leg parameters, it is possible to achieve stable pitch behavior for trotting quadrupeds. However, the effects of roll and yaw on the stability of the robot could not be neglected.

The trot is a two-beat gait that has a wide variation in possible speeds and averages about 13 km/h for a horse. It is the working gait for a horse. Despite what one sees in movies, horses can only canter and gallop for short period at a time, after which they need to rest and recover [35]. Horses in good condition can maintain a working trot for hours. The trot is the main way horses travel quickly from one place to another [35]. Although many animals gallop at top speeds, there is a significant range of intermediate speeds for which trotting is the most energy efficient gait [40, 41]. For these reasons, we are highly interested in the trot gait rather than a faster gallop.

Contribution

Legged robots have many degrees of freedom compared to wheeled robots. This requires_more actuators and sensors to control the extra degrees of freedom. Several

researchers are looking into the use of under-actuated compliant legs to reduce the complexity.

How much stability can be provided through properly designed passive legs? We propose that by properly designing compliance, stability can be improved passively, which in turn increases the robustness of the robot. An analogy is that of an airplane. A controller can stabilize an aerodynamically unstable plane, but an aerodynamically stable airplane is more robust in its flying stability.

In this work we present a quadruped model that requires only two motors to navigate. Thus, it is possibly more energy efficient. Velocity profiles are provided to the motors to match the characteristics of the trot gait and desired speed.

A goal for this paper is to stabilize the robot trotting, and secondly, to minimize the absolute maximum and RMS of the roll, pitch and yaw in a trotting small sized robot. It is also desired to explore the body attitude of a quadruped robot while trotting at high speeds.

Palmer and Orin [42-44]; were able to achieve trotting speed of 5.25 m/s for a horse sized robot, approximately four body lengths per second, by utilizing a very complex control algorithm. Their quadruped weighed a total of 76 kg and stood 60 cm high with the knee springs in their nominal position. The shoulder separation was 35 cm and the shoulder-to-hip distance was 1.2 m. By passively actuating the legs due to desired velocity profiles, and utilizing appropriate leg stiffness, we were able to achieve maximum stable trotting speed of 2.37 m/s for a small dog sized robot, approximately eight body lengths per second. No feed-back or feed-forward control algorithm was used on this experiment.

Palmer and Orin's robot was able to maneuver over uneven terrain with standard deviation of height variation of 3 cm at 4.0 m/s (maximum terrain elevation of 6.5 cm, which was greater than 10% of the nominal leg length). However, they used panels to model the uneven terrain. Each floor panel was 60 cm in length (almost half of the robot's length). The elevation of each panel was randomly selected from a normal distribution, resulting in a highly smooth change in elevation.

Our trotting robot model is able to overcome disturbances in the form of step and hole with the height and depth of 6% of the body's height, respectively. The disturbance was applied to the robot after a few full stride cycles. The robot's right fore leg stepped into a hole (stepped on a stair) while trotting at 1.73 m/s, approximately six body lengths per second. The robot showed less capacity to overcome disturbances, compared to Palmer's robot, but it should be noted that no control algorithm was used to return the robot to balance and the robot was able to maintain balance passively.

It is interesting to note that Herr and McMahon [7] in their modeling of a horse with pogo-stick compliant legs could not achieve acceptable pitch control with passive compliance alone. Meek et al. [16] demonstrated that it is possible to achieve passive pitch control in 2D with passive anisotropic compliant legs. In this work we show that not only passive pitch, roll, and yaw control is obtainable through a proper compliance design of an under-actuated compliant leg, but also; the absolute maximum of roll, pitch and yaw would be very negligible (smaller than 3°) in the course of trotting.

This appears to be the first 3D analysis of a trotting quadruped robot that utilizes passive under-actuated compliant legs. We show that stable trotting is achievable without

using any control algorithm. Moreover, the robot is able to passively maintain balance after encountering disturbances.

CHAPTER 3

MODELS

We hypothesize that stability could be achieved through proper design of the leg compliance. To test our hypothesis, a computer model was generated using MATLAB/Simulink and SimMechanics toolbox [17]. This software uses relative coordinate formulation along with numerical integration to solve the equations of motion [18]. Since the problem is suspected to have stiff differential equations, numerical integration was performed using ODE15S, which is an implicit continuous variable-step solver based on the numerical differentiation formulas (NDFs) and numerical evaluation of Jacobian matrix [19]. This solver is used to solve stiff differential equations with the highest accuracy among all the solvers that MATLAB offers. It is also recommended that this solver should be used as the primary solver when dealing with stiff ODEs.

Multibody Quadruped Model

The dimensions and mass properties of the model, which are based on the biological model [16], roughly correspond to the dimensions and mass properties of a small dog (Table 1). Body is presented as a cuboid with shoulder to shoulder distance of 0.11 m and hip to shoulder distance of 0.3 m. Shoulder and hip height were 0.23 m to match the values of previous work [11]. Mass of the body is 5.7 kg and it is distributed

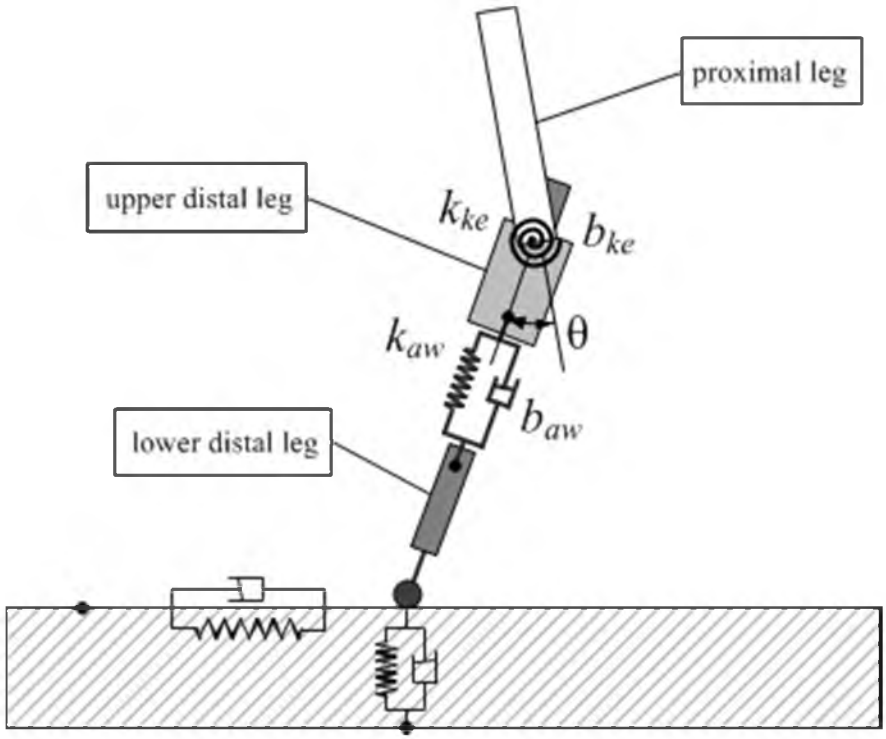

Fig. 2 - Model of an individual leg

homogeneously along the body. Together, all four legs (two fore legs and two hind legs) represented about 10% of the total body mass [24]. It is desired to investigate the effect of realistic legs on the stability of trotting.

Each leg has 4 degrees of freedom, and comprised three segments: a proximal segment, an upper distal segment, and a lower distal segment with a foot. A prismatic joint and a translational spring with stiffness k_{aw} and damping b_{aw} were assigned in between the lower and upper distal portion of the leg. Together, the distal segments function like a pogo-stick. Such compliant prismatic joints have been used in most quadruped robots that are capable of running [1, 7- 9, 11, 14-16]. Actuation of this prismatic joint would provide leg clearance during flight phase. This distal leg joint is referred to as the ankle on the hind leg and the wrist on the fore legs.

Table 1. Parameters of the robot's body and legs

		Mass (Kg)	Length (m)	Width (m)
Body		5.7	0.3	0.11
proximal		0.05	0.1	N/A
Distal	upper	0.05	0.075	N/A
	lower	0.05	0.075	N/A

The second degree of freedom is a revolute joint between the upper distal and proximal segment of the leg supported by a torsional spring with stiffness k_{ke} and damping of b_{ke}. These would be referred to as the knees and the elbows. The first reason for including compliant knee and elbow is that simple pogo-stick legs can impose kinematic constraints when used in trotting gait because they have only one DOF below the hip [25, 26]. Lee and Meek presented that the addition of this joint would provide a solution to this problem by permitting a pair of contact legs to lengthen and shorten freely (allowing unactuated pitch-axis rotation about the elbow or knee) [11]. Another objective is to provide the leg configurations presented in [16]. Through multiple simulations of the robot, Meek et al. [16] suggest that caudal inclination of humeri and cranial inclination of femora (Fig. 3-b), matching with most high speed mammals, is the best configuration for minimizing pitch behavior. This configuration referred to as "natural" configuration, along with knee elbow angle of 30° (Fig. 3-b) was chosen as the default leg posture. Later on, this assumption is assessed. After investigating proper values of leg parameters that would minimize the body's pitch, roll, and yaw, the same optimized values of leg parameters are used on three different models. These models that utilize different leg configurations in sagittal plane (Fig. 3-c), referred to as "reverse," "backward," and "forward" postures are tested with the same leg parameters to investigate the advantage

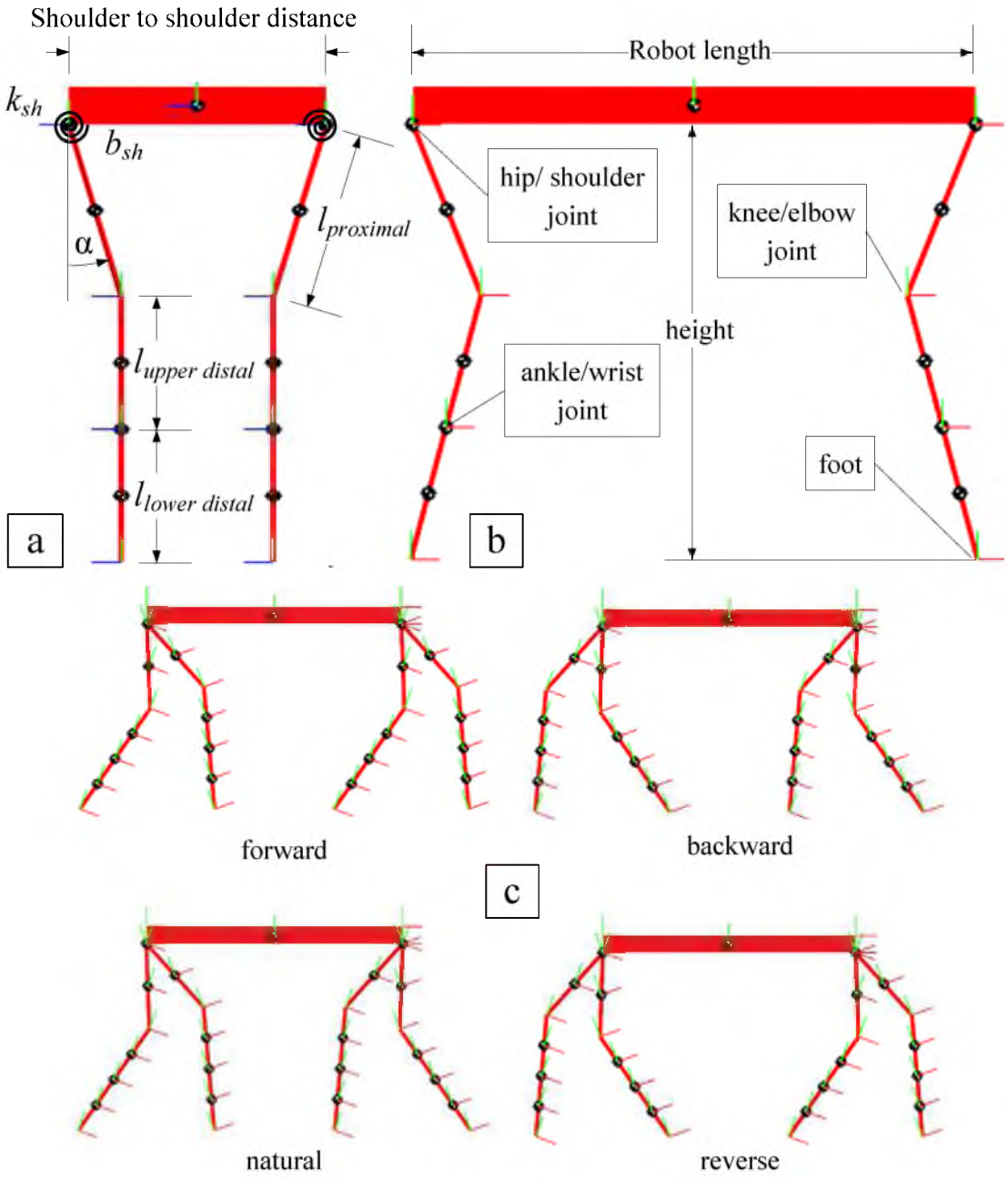

Fig. 3 – Quadruped robot model (a) The robot in sagittal plane (b) Robot in frontal plane. Alpha is the angle between proximal portion of the leg and vertical line. The positive direction for alpha is defined as counter clockwise for the left fore-leg.

of each leg configuration over another. One-dimensional Poincaré maps of states of the body are used to explore the best configuration, and a brief discussion is presented in Chapter 4.

The hip and the shoulder are attached to the body by two perpendicular revolute joints. The first one is normal to the sagittal plain and is directly actuated by the motors. Another pin joint perpendicular to the frontal plane and intersecting the shoulder joint (Fig. 3-a) is included to investigate the effects of alpha (i.e., the angle between proximal portion of the leg and vertical line in frontal plane (Fig. 3-a)) on robot performance. A torsional spring with stiffness k_{sh} and damping of b_{sh} is utilized to passively support this degree of freedom. The addition of this joint is based on the supposition that through deviating the ground forces from the sagittal plane, it is possible to manipulate the roll behavior of trotting. We predicted that the resultant ground reaction force vector exerted to the body trunk would tend to align with the direction of alpha.

Feet were modeled as points with no geometrical extension. Stiffness and damping of the torsional spring-dampers augmented in knee/elbow and hip/shoulder joints in addition to the linear springs and dampers of the ankle and the wrist are to be regulated to achieve the desired compliance. These parameters as well as alpha and stride length are tuned to accomplish maximum performance in a designated speed correspond with the desired Froude number. Three speeds were selected. One at the start of the trotting range corresponding with the Froude number of 0.5, another one in the middle of the range relating to the Froude number of 1.2, and finally at the end of trotting range with the Froude number of 2.5.

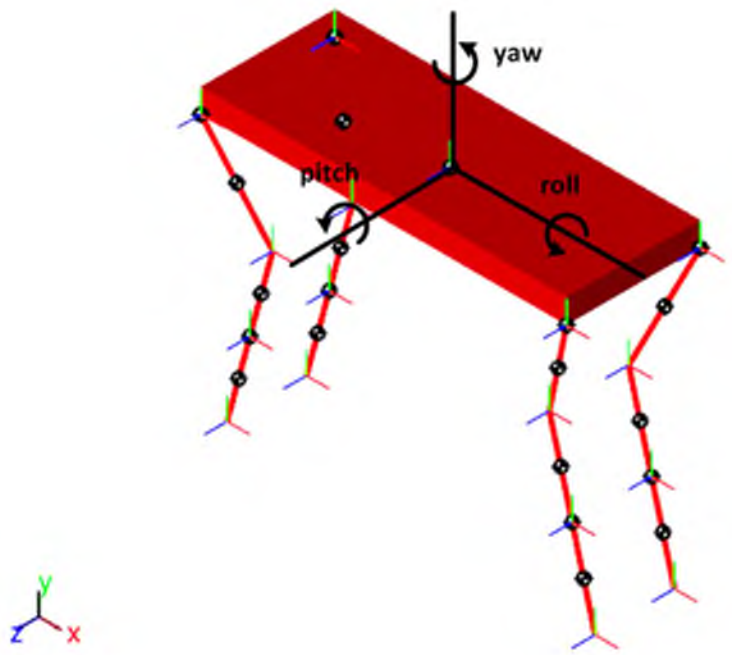

Fig. 4 – Quadruped model and the global coordinate system. Roll, pitch, and yaw are shown in the picture.

Ground Collision Modeling

The ground was represented with linear springs and dampers in the vertical and horizontal directions to model the viscoelastic properties of the surface. Ground stiffness in the vertical direction was set to 100 (kN/m) and damping was set to 10 (kN-s/m). It was desired to make the ground very rigid and to lessen the coefficient of restitution to about zero. Coefficient of restitution of zero would guarantee minimal oscillations between foot and ground. Several researchers have used ground stiffness in the range of 75 – 400 kN/m [7-8, 42-44].

A compliant ground in the x and z direction was required so that each foot would not slip (Fig. 2). Spring and dampers in the horizontal directions were set to one hundredth of the vertical stiffness and damping, respectively. Using such ground stiffness

each foot deflects the springs in the x direction approximately 2 mm, 0.5 mm in the y direction, and 0.1 mm in the z direction. Using stiffer ground is not recommended because it makes the trotting unstable by applying too much braking force to the front feet at the moment they touch the ground.

Feed-forward Control

In a trotting gait, the right front leg is retracted with the left rear leg and the left front leg is retracted with the right rear leg. The two diagonal pairs are a half cycle out of phase, producing an alternate pattern of diagonal foot contact. Simulations start with an initial stride length (i.e., the angle each leg sweeps during a stride phase which is equal to the angle it sweeps during a flight phase, symmetrical about the vertical line in the sagittal plane), and an initial stride period. Afterwards, stride length is varied to investigate its effect on the stability of the robot. Different velocities were also tested. Simulations start with Froude number of about 1, which is almost in the middle of the trotting range. The average forward velocity for this simulation was 1.7 (m/s), which is about 5.7 body lengths per second. Other simulations were performed on the high and low ends of the trotting region.

A motor at each shoulder and hip controlled the angular velocity of the leg by applying the requisite torques. A feed-forward controller was implemented to retract the legs at a constant angular velocity of 445 (1°/s) during stance phase. This angular velocity corresponds with the desired forward speed of the body. At the end of this phase the actuator on the prismatic joint retracts the ankle and wrist joints of the legs that have reached the end of the stride phase. This shortens the legs, providing desired leg

clearance and preparing the leg for the flight phase. During flight the leg protracts with the same angular velocity, but in the opposite direction. Before reaching the end of flight phase, the actuators on the ankle and wrist would extend the lower distal leg towards the ground. The leg is fully extended before it reaches the end of flight phase. This strategy would ensure leg retraction just prior to foot contact (start of next period), referred to as ground speed matching. [27] This is quite common during fast locomotion of mammals. [28]

As illustrated by the actuation signals of Fig. 5, a tabular feed-forward controller was used to control the velocity and position of the shoulder/hip joint together with those of the ankle/wrist joint in a period of 0.2 (s). While the hip and shoulder were subject to feed-forward control, the legs behaved passively during stance and flight. It is important to identify that the retractor-extender actuator augmented at the wrist and ankle is only active in half of the period, all through the flight phase. The leg is supported by the compliance throughout the stance.

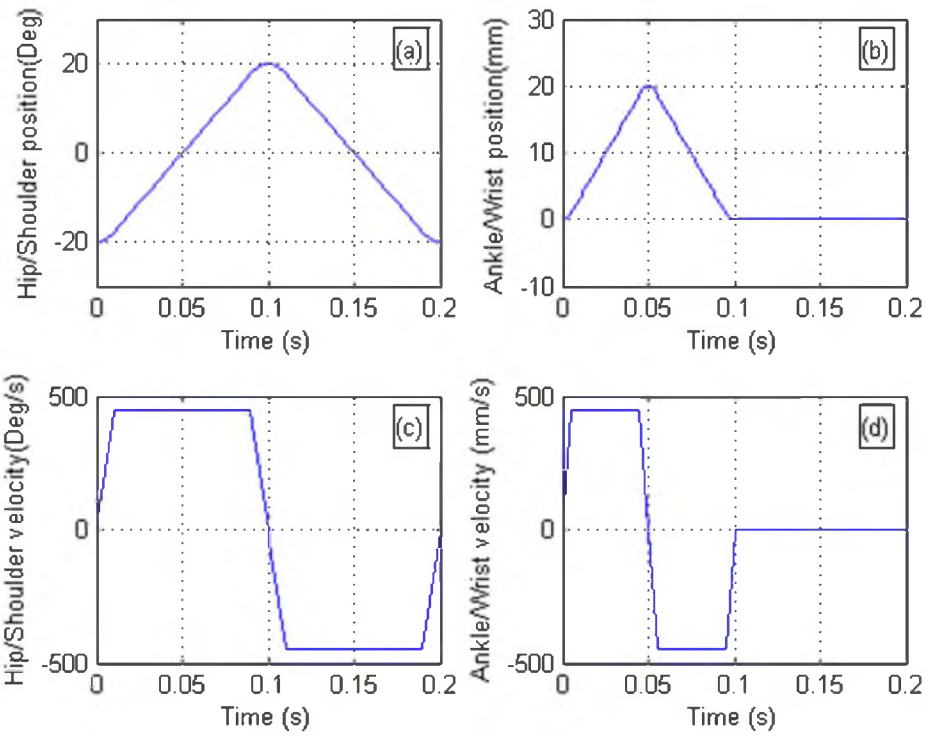

Fig. 5 - Position and velocity signals sent to the hip/shoulder and ankle/wrist joints (a) Front right shoulder position in a period T= 0.2 (s). Front right leg is initially at the end of stride phase θ = -20°. (b) The front right wrist would retract to provide leg clearance during flight phase. (c) The shoulder would reach to θ = 20° which is the beginning of the stance phase. (d) The wrist would extend towards the ground before shoulder angle (θ) reaches to 20°

CHAPTER 4

SIMULATION RESULTS

Given the large number of degrees of freedom in the quadruped model, and the nonlinear nature of trotting, analytical solutions were not practical in this study. Instead, realistic computer simulations were performed to examine the attitudinal behavior of a high speed trotting machine. The laws of Newtonian physics were applied to the rigid bodies coupled together by joints. The trunk was not constrained by any means, letting the body to move in any direction and rotate freely about its principle axes. Furthermore, we predicted that the effect of rolling and yawing on the stability of trotting must not be ignored.

The responses consist of two phases: a transient response and a steady state response that was achieved typically within two or three steps. The ground was modeled flat in the steady state response simulations. Trotting starts with an initial velocity in the forward direction. The reason is to dispose of gait transition effects which are not the focus of this research. Secondly, it is desired to start the simulation from a steady condition. The initial velocity is always slightly higher than the mean forward velocity. This is expected because the forward velocity of a spring-loaded inverted pendulum (SLIP) reaches a maximum during flight phase [26].

The increase in stability was determined by decrease in roll, pitch, and yaw motion. Given that, the robot can rotate in positive and negative directions, the absolute maximum of each rotating angle along with root mean square (RMS) of the data in one simulation was obtained and compared to the other simulation results to evaluate the competitive advantage of each design. The simulation would stop if the roll or pitch angle of the robot trunk exceeds 70°. This constraint was added to the simulation because the robot would not be able to maintain balance after such abnormal deviations in the roll and pitch. A Poincaré map of each state was also monitored to ensure stable trotting. The parameters that were varied were the ankle/wrist spring constants, the knee/elbow and hip/shoulder spring constants, α, stride length, distal leg retraction lengths, and the velocities of the robot.

Also, it is desired to match the vibrational characteristics of the different models. This was done by matching the damping ratio of the legs for all variations of the leg parameters. The attenuation rate $R_{k/d}$ was introduced as the ratio of damper constant b and spring stiffness k, using the equation:

$$R_{k/d} = \frac{b}{k} \tag{2}$$

Because mass properties of the body and the legs are constant throughout the simulation, damping ratio would also be constant throughout the simulation. Knowing the mass of each segment of the leg and the body, one can easily relate the attenuation rate to damping ratio.

The parameters' search space is large. To effectively find the values that would minimize the rotations of the main body a simple but efficient strategy was employed. Firstly, we altered each parameter to find the stable range of trotting entitled to the specific parameter, and subsequently we varied the parameter values in the stable range simultaneously to find the absolute minima.

It is interesting to note that Herr and McMahon [7] in their modeling of a horse with pogo-stick compliant legs could not achieve acceptable pitch control with passive compliance alone. Meek et al. [16] demonstrated that it is possible to achieve passive pitch control in 2D with passive anisotropic compliant legs. In this work we show that not only passive pitch, roll, and yaw control is obtainable through a proper compliance design of an under-actuated compliant leg, but also, the absolute maximum of roll, pitch and yaw would be very negligible (smaller than 3°) in the course of trotting. A series of screen captures for one stride of the trotting gait is given in Fig. 6, showing biological features like diagonal legs movement, stride and flight phase for every leg, and a smooth gait with minimum roll, pitch, and yaw motion.

Figure 7 shows the trotting quadruped from the side view. It shows that at a point during the trot, all four legs of the quadruped are off the ground. At time equal to 0.44 seconds, all four legs of the trotting quadruped are off the ground.

Leg parameters were initially set to the values that match the results of quadruped trotting analysis in 2D [16]. Distal spring was set to 3 (kN/m), knee/elbow spring was set to 1 (N·m/deg), and theta was set to 30°. Starting with hip/shoulder stiffness and varying it in a wide range, an optimal value was found for each parameter. The optimal values were used instead of initial values afterwards.

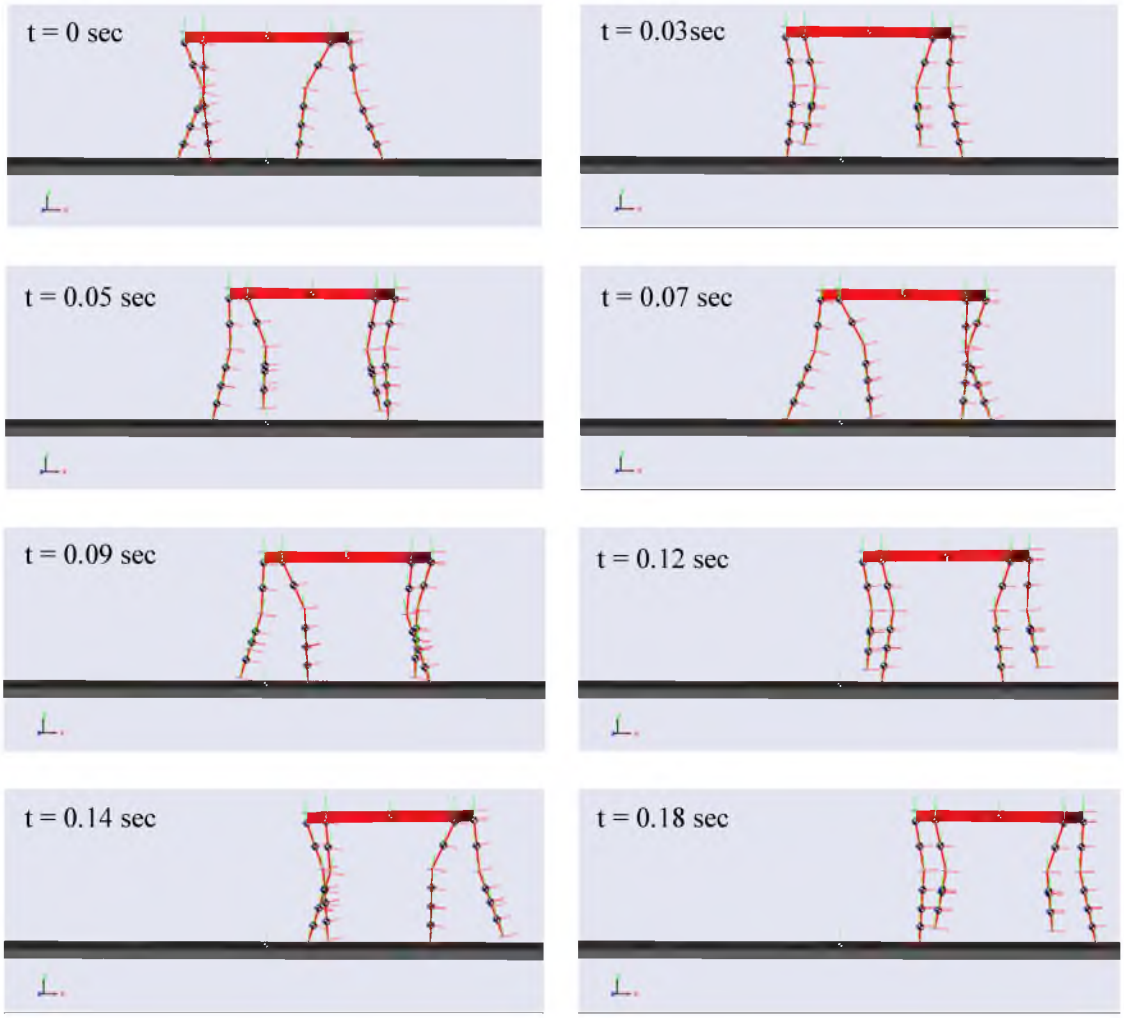

Fig. 6 – Screen captures of 3D trot over one stride.

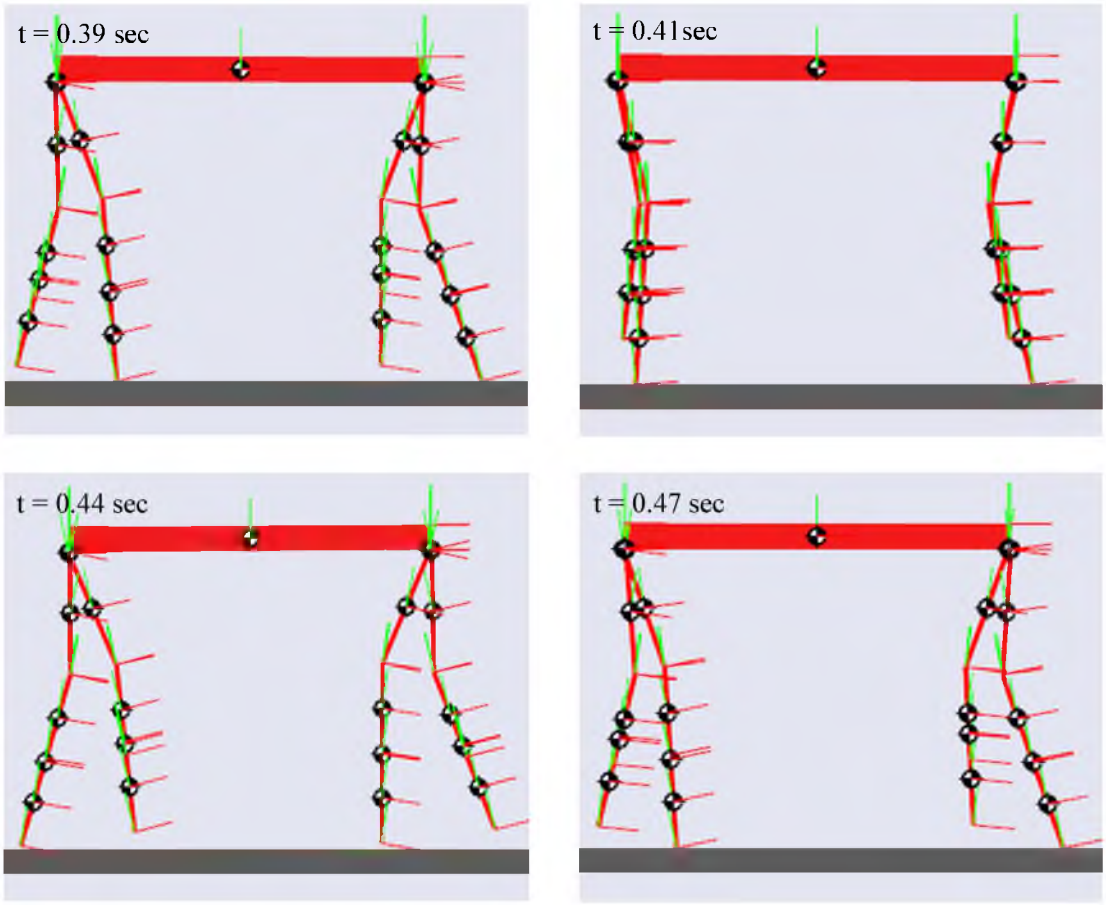

Fig. 7 – Screen captures of 3D trot from side view.

The effect of the fallowing parameters on the stability of quadruped trotting was examined:

Hip/Shoulder Stiffness

Changing the hip and shoulder stiffness from 0.01to 100 (N-m/deg) revealed that, the stiffer the torsional spring at the hip and shoulder becomes, the more stable the robot will be (Fig. 8). This was performed while keeping all the other parameters constant. The same results were obtained with different alphas (i.e., the angle of the proximal leg segment with the vertical line in the frontal plane). This interesting result would cause the elimination of the hip and shoulder compliance. As a matter of fact, rigid joints could be used in the actual design of the robot. This is consistent with leg designs implemented in most of the quadrupeds capable of trotting and bounding [7]-[16].

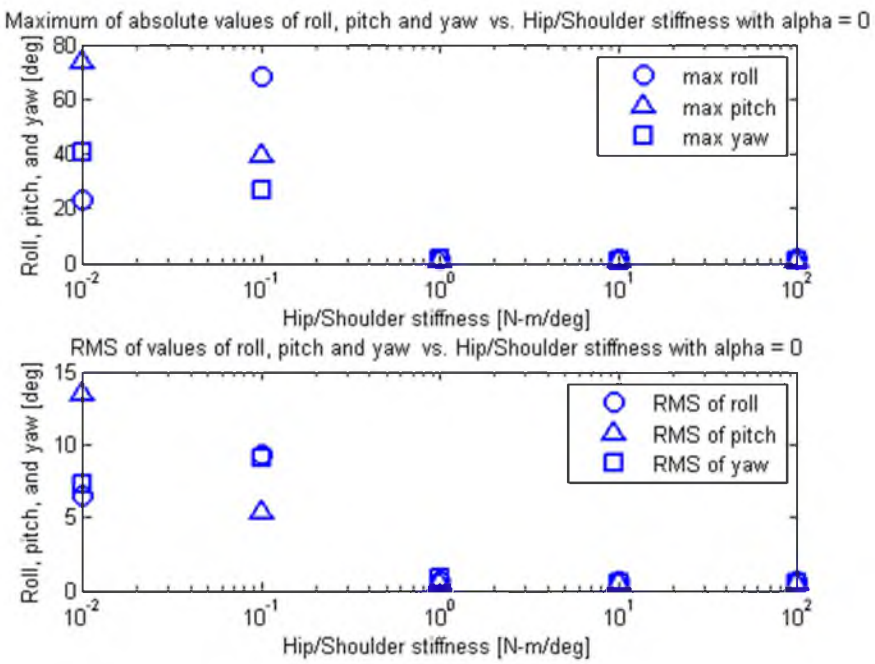

Fig. 8 - The effect of the hip and shoulder stiffness on the maximum and RMS values of roll, pitch, and yaw for alpha = 0°.

A hip and shoulder stiffness of 10 (N m/deg), which is a very stiff spring constant comparing to the masses of legs and body, was used from this point on. It is important to note that by checking the maximum values of roll, pitch, and yaw, one can easily discover whether the robot is adopting a stable behavior or if it suffers from unstable attitude throughout the simulation. It was mentioned before that a constraint would stop the simulation if any of the values of the roll and pitch goes higher than 70°. The addition of this constraint makes the simulations much more time efficient because the robot would not be able to restore balance after this point.

Alpha

The angle of the proximal leg segment with the vertical line in the frontal plane, alpha (Fig. 3-a), was varied from -20° to 8°. The positive direction for alpha is assumed counter clockwise for the left fore-leg. The quadruped starts to grow unstable attitude as the alpha shifts into positive values (Fig. 9). This happens because the distance between the ground contact point of the feet of fore-legs and those of the hind-legs would become small. An alpha in the range of -11° to -14° appears to have the minimum roll and yaw (Fig. 9); thus, -13° was chosen as the ideal alpha.

Figure 9 also illustrates that the maximum pitch angle occurring throughout the simulations is almost constant for a wide range of alpha. For the values of alpha between 2° and -14°, the change in maximum pitch angle is less than half a degree.

Knee/Elbow Stiffness

Several knee and elbow stiffness were applied to the model to investigate the effect of upper distal leg's compliance on the overall performance of the robot. Initially,

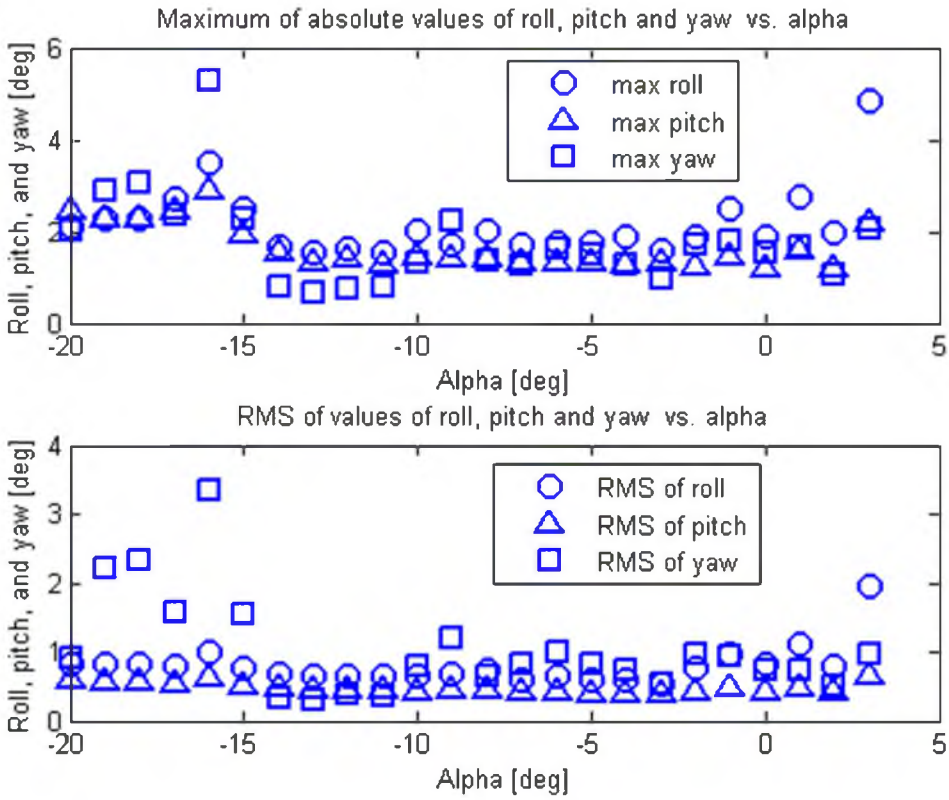

Fig. 9 - The effect of alpha on the maximum and RMS values of roll, pitch, and yaw. Alpha is varied between -20° - 3°. The positive direction of alpha is defined as counter clockwise for the left fore-leg

it was varied between the range of 0.01 to 100 (N·m/deg). It appears that unlike the hip and shoulder stiffness, changing the knee and elbow stiffness would result in a minimum attitudinal roll, pitch, and yaw throughout the simulation (Fig. 10). A closer look at data achieved from simulation (Fig. 10) revealed that the best performance was achieved utilizing a stiffness of 0.1 (N·m/deg), which is considered a fairly soft spring. This is consistent with the results of previous work on 2D trotting [16] in which a soft knee/elbow spring was suggested to achieve minimal pitch. Values of less than 0.075 (N-m/deg) are considered to be too much soft and will drive the robot unstable. After 0.15 (N-m/deg) the values for maximum and RMS of roll, pitch, and yaw will start to grow once again.

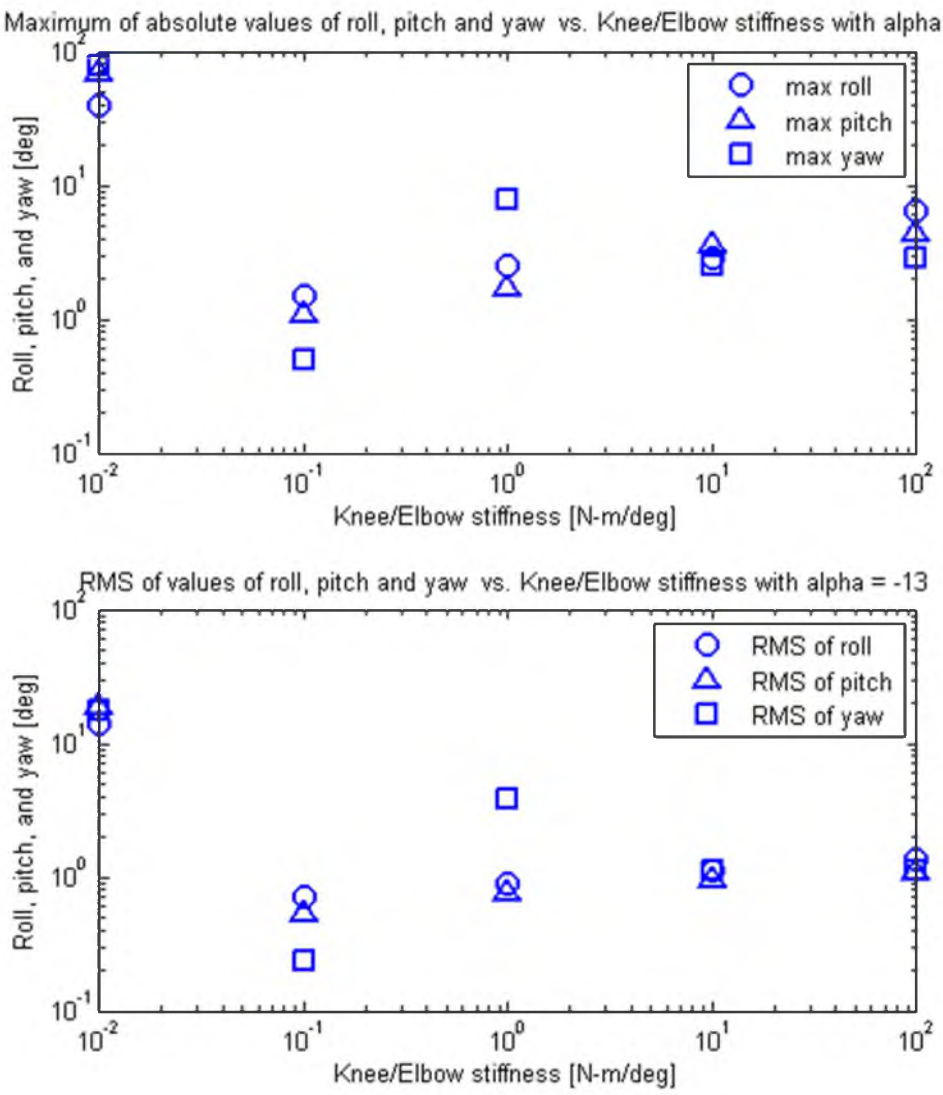

Fig. 10 - The effect of the knee and elbow stiffness on the maximum and RMS values of roll, pitch, and yaw for alpha = -13°. Range of the knee/elbow stiffness is 0.01 – 100 (N-m/deg) on a logarithmic scale.

Ankle/Wrist Stiffness

Firstly, ankle and wrist stiffness were varied in the range of 1-100 (kN/m). The results obtained from multiple simulations are presented in Fig. 11. Results demonstrated that the trotting is stable for a wide range of stiff springs and unstable for soft springs. For the values of 1000 N/m and less, the robot adopts unstable attitude. A quick calculation indicates that a spring with stiffness of 1000 (N/m) attached to a mass of 3 (kg) (i.e., a robot that weighs about 6 kg, divided by two; because the mass is distributed on two legs throughout the course of trotting) would deflect the spring less than 3 cm. It should be noted that the impact of the foot to the ground may result much higher forces and deflections on the spring that is ignored in the calculations.

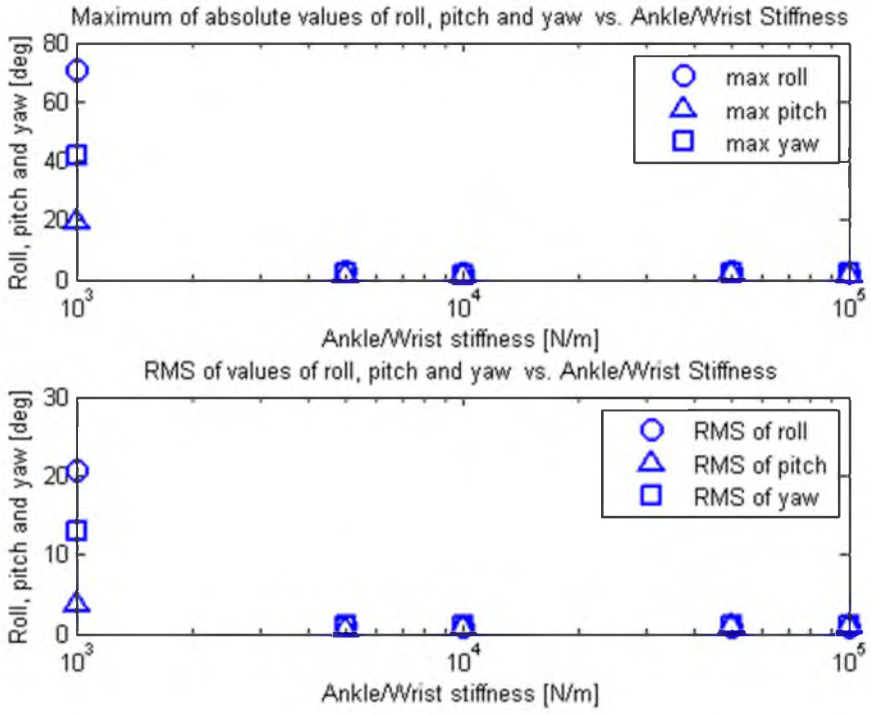

Fig. 11 - The effect of ankle/wrist stiffness on the maximum and RMS values of roll, pitch, and yaw. Range of the ankle/wrist stiffness is 1 – 100 (kN /m) on a logarithmic scale.

Secondly, ankle and wrist stiffness were varied in the range of 1-10 (kN/m) to get a better understanding of the point in which robot tends to go unstable and if there exist a local minimum (Fig. 12). Soft springs tend to make the robot trotting unstable. Furthermore, stiffer lower distal leg springs minimize the roll, pitch, and yaw attitude of the robot. Stiffer springs as high as 100 (kN/m) were also applied to the ankle and wrist, resulting in a good performance as well.

A closer look at the ranges 2-8 (kN/m) revealed that the roll, pitch, and yaw throughout the simulation is minimum while the ankle and wrist stiffness is 6 (kN/m). This value, which is very common in commercial products, was chosen as the standard value of the ankle and wrist stiffness from this point forward.

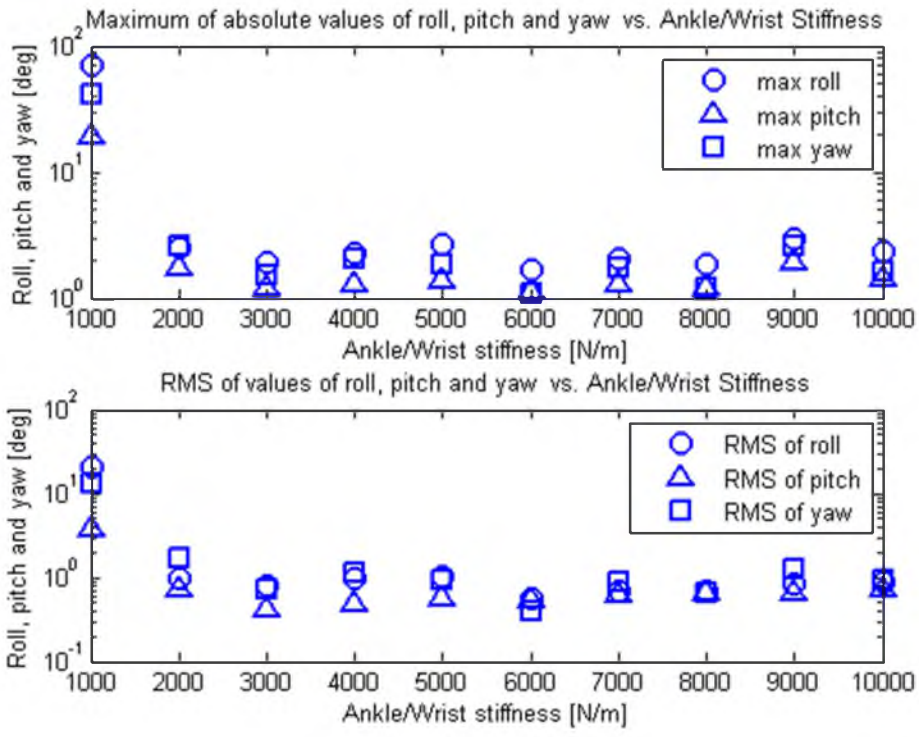

Fig. 12 - The effect of ankle/wrist stiffness on the maximum and RMS values of roll, pitch, and yaw. Range of the ankle/wrist stiffness is 1 – 10 (kN /m)

These results also match previous 2D trotting results [16], in which a stiff spring at the lower distal leg of the quadruped was suggested to result in a better pitch performance. We added that a stiff ankle and wrist spring would also minimize the roll and yaw of the quadruped trotting.

Attenuation Rate

Attenuation rate ($R_{k/d}$) was utilized to match the vibrational characteristics of all the springs in the model. This parameter was varied in the range of 0.1-0.7 (s). The robot had a more stable trotting with lower attenuation rates rather than higher ones (Fig. 13). Since $R_{k/d}$ is defined as the ratio of damping over stiffness for all springs, smaller $R_{k/d}$ corresponds with smaller damping ratios. Damping ratio is not needed in this problem because mass is constant. If the foot is touching the ground, the springs are bearing the whole mass of the robot, but during the flight phase the mass of the whole leg is acting on the hip/shoulder springs. The knee/elbow springs tolerate the mass of the whole distal leg, and the ankle/wrist springs only endure the mass of lower distal leg.

Stride Length

Stride length was varied between 10° to 80° which is equivalent to ±5° to ±40°; all symmetric about 0° (i.e., the 0° is defined as the vertical line in sagittal plane intersecting the hip or shoulder joints). Changing stride angle does not have an effect on the angular velocity of the leg. Results are presented in Fig. 14.

Stride lengths of ±15°, ±20°, and ±25° appear to minimize the roll, pitch, and yaw, despite the fact that smaller stride angles could also result to stable trotting but with higher fluctuations in the roll, pitch, and yaw.

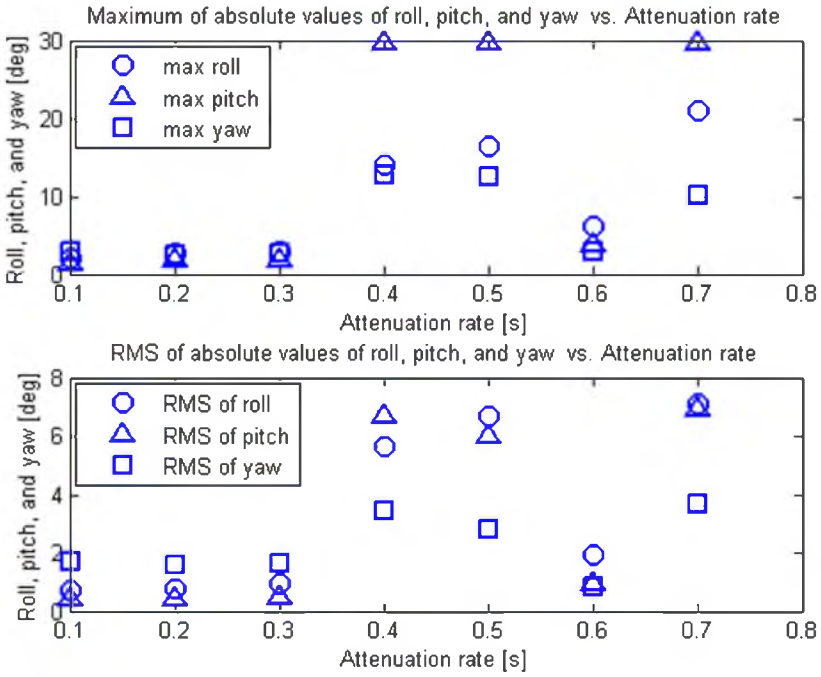

Fig. 13 - The effect of different attenuation rates on the maximum and RMS values of roll, pitch, and yaw.

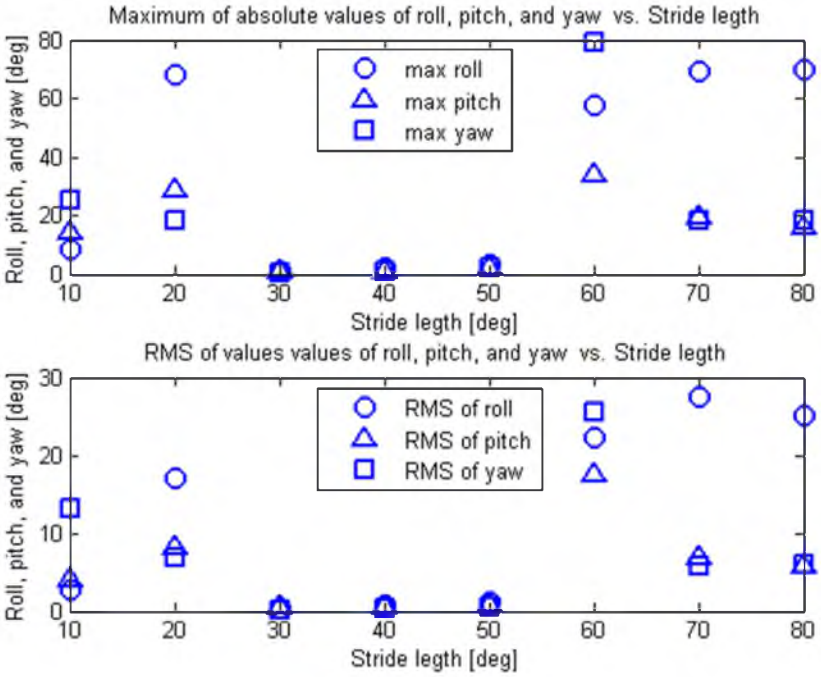

Fig. 14 - The effect of stride length on the maximum and RMS values of roll, pitch, and yaw.

Hind to Fore Leg Ratio

Hind to fore leg ratio is defined as the ratio of the ankle stiffness over wrist stiffness. The robot suffers from "nose-up pitch" problem especially while operating with gaits such as bounding. Nose-up pitch is when the quadruped suffers from constant positive pitch during its running course. In order to counteract this problem, it is often suggested that a stiffer spring should be used in the ankle rather than that of the wrist [11, 16, 20]. A dimensionless parameter is introduced:

$$Hind\ to\ fore\ leg\ ratio = \frac{k_{ankle}}{k_{wrist}} \tag{3}$$

in which; k_{ankle} is the ankle stiffness and k_{wrist} is wrist stiffness.

Results represented in Fig. 15 verify previous findings in [16]. It appears that for the values of one and higher, results do not dramatically change. As a result, the hind to fore leg ratio of one was chosen for this robot.

Leg Configurations

Simulations were performed using different leg configurations in sagittal plane in order to find the best leg configuration. Four diverse models were constructed varying only in the direction of the knee and the elbow inclinations. The configuration with both the knee and elbow pointing forward (i.e., in the direction of locomotion) is referred to as "forward", and the contrariwise posture is referred to as "backward" (Fig. 3-c). The biological model is the one with the knee forward and the elbow pointing backward. This was referred to as the "natural" configuration in Fig. 16. The inverse of natural posture is referred to as "reverse."

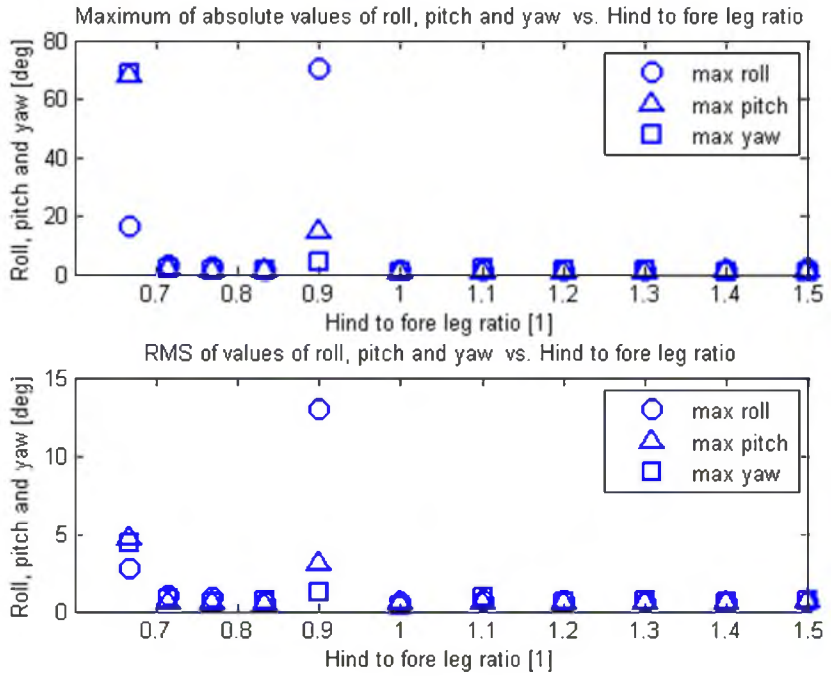

Fig. 15 - The effect of hind to fore leg ratio on the maximum and RMS values of roll, pitch, and yaw.

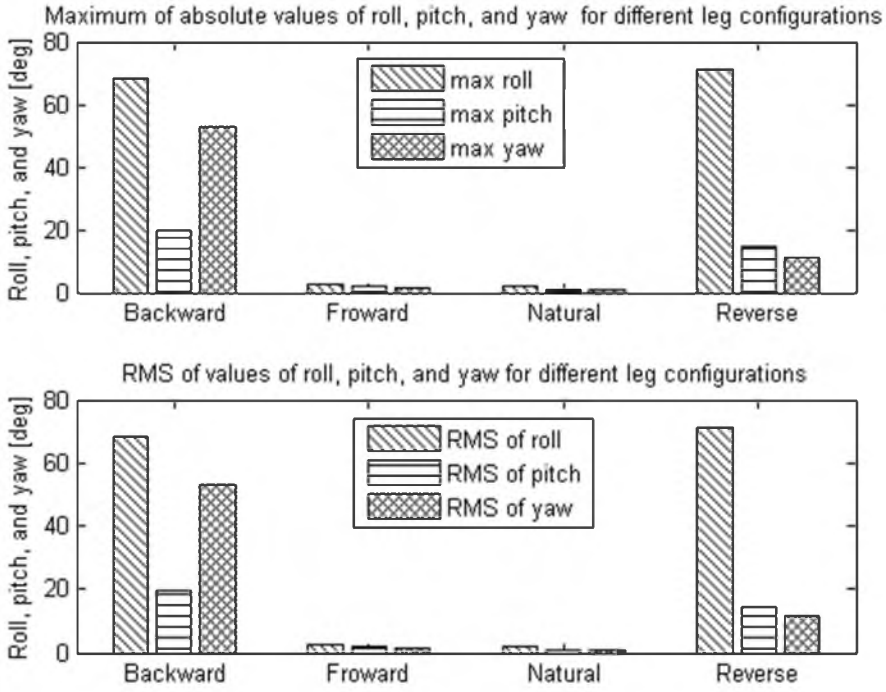

Fig. 16 - The effect of different leg configurations on the maximum and RMS values of roll, pitch, and yaw.

The reverse and backward configurations result in unstable trotting while the forward and natural postures are perfectly stable. As a result for design purposes, the elbows should always point backward. After comparing the maximum and RMS values of roll, pitch, and yaw it is revealed that the natural configuration still has the best performance [16].

Theta

Theta, the supplementary angle of the angle between proximal and upper distal section of the leg (Fig. 2), was varied between 0° to 50°. The leg with 0° theta is the simple pogo-stick leg found in previous works. Simulations were performed using different thetas on the model with the natural leg configuration. Results illustrate that although the robot with pogo-stick legs is stable, fluctuations of the roll, pitch, and yaw are not the lowest possible. Using a theta of 20° on the biological leg configuration appears to have the best results. The models utilizing thetas of equal to and greater than 50° appear to have unstable trotting behavior.

The list of parameters, their ranges and optimal values are summarized in Table 2.

Poincaré Maps

Poincaré maps of the roll, pitch, and yaw for previous leg configurations are presented in Fig. 18-21. The maps are generated for each state using the angular velocity of the right fore leg in terms of its angle, every time the right fore leg touches the ground (e.g. roll angular velocity of the right fore leg at the moment it hits the ground with respect to the roll angle at that moment). Each discrete point represents the velocity with respect to the associated angle in time. In order to achieve a better understanding of the

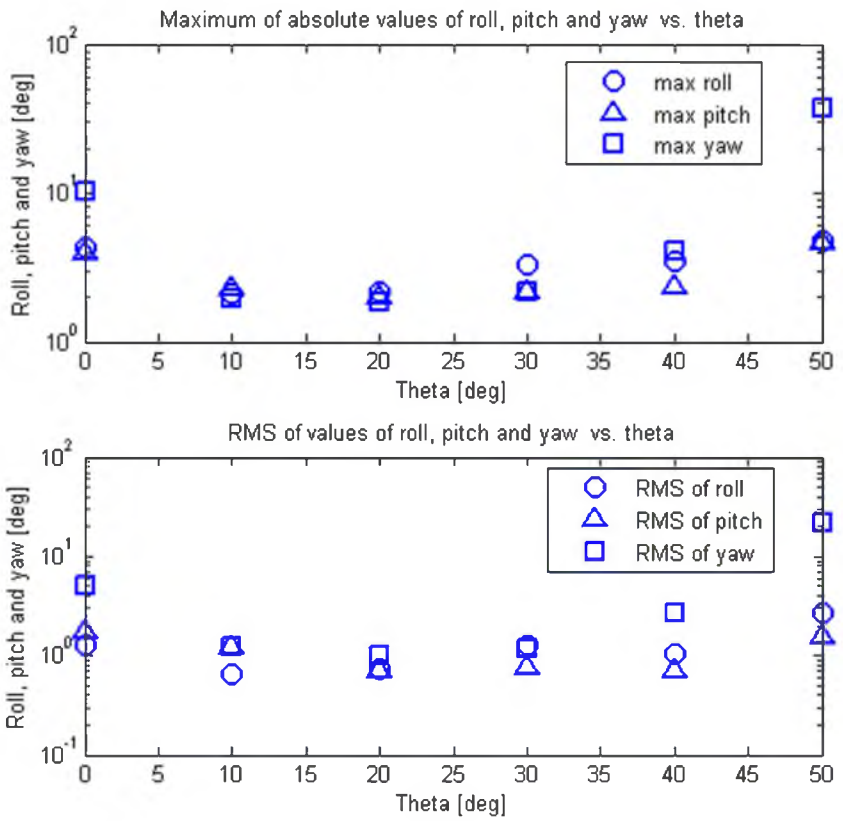

Fig. 17 - The effect of theta of natural leg configuration on the maximum and RMS values of roll, pitch, and yaw.

Table 2. List of parameters, their ranges and optimal values for steady-state analysis

Variable Name	Symbol	Range	Optimal Value
Hip/Shoulder Stiffness	k_{hs}	0.01-100 (kN-m/deg)	10 (kN-m/deg)
Alpha	α	-20°- +8°	-13°
Knee/Elbow Stiffness	K_{ke}	0.01-100 (kN-m/deg)	0.1 (kN-m/deg)
Ankle/Wrist Stiffness	K_{aw}	1–100 (kN /m)	6 (kN /m)
Attenuation Rate	$R_{k/d}$	0.1-0.8 (s)	0.1 (s)
Stride Length		10°- 80°	30° (±15°)
Hind to Fore Leg Ratio		0.67 – 1.5	1
Theta	θ	0°- 50°	20°

stability, each point is connected with a straight line to the next point in time. If the dots spiral in toward a point, the trotting is stable. If they spiral out, it shows instability, and a circular pattern represents marginal stability. The area that the dots occupy provides a rough estimation of the amount of stability that the robot has achieved throughout the course of trotting.

Fig. 18 illustrates the Poincaré maps of the roll, pitch, and yaw for the robot with backward leg configuration, and Fig. 19 represents the same Poincaré maps for the robot performing with the forward leg posture. Fig. 20 speaks for the natural leg posture and finally, Fig. 21 corresponds to reverse leg configuration.

As stated previously, the trotting robot that employs backward leg configuration is unstable. The maps perfectly validate previous results. The maps of roll, pitch, and yaw utter the fact that the plots of all states spiral outward. On the other hand, the plots associated with forward configuration illustrate the fact that backward configuration that has been employed in some of the previous robots, demonstrate stability. It can also be concluded from the plots that the natural configuration is more stable than the backward posture.

Different Trot Speeds

After successfully implementing a stable trotting quadruped operating in a Froude number of 1.2, the robot model was tested in two other speeds in the lower and higher range of trot. Quadrupeds change their walking gait to trotting at Froude number of 0.5 and change from trot to gallop at Froude number of 2.5. These two values were chosen to test the previous optimal values in different speeds.

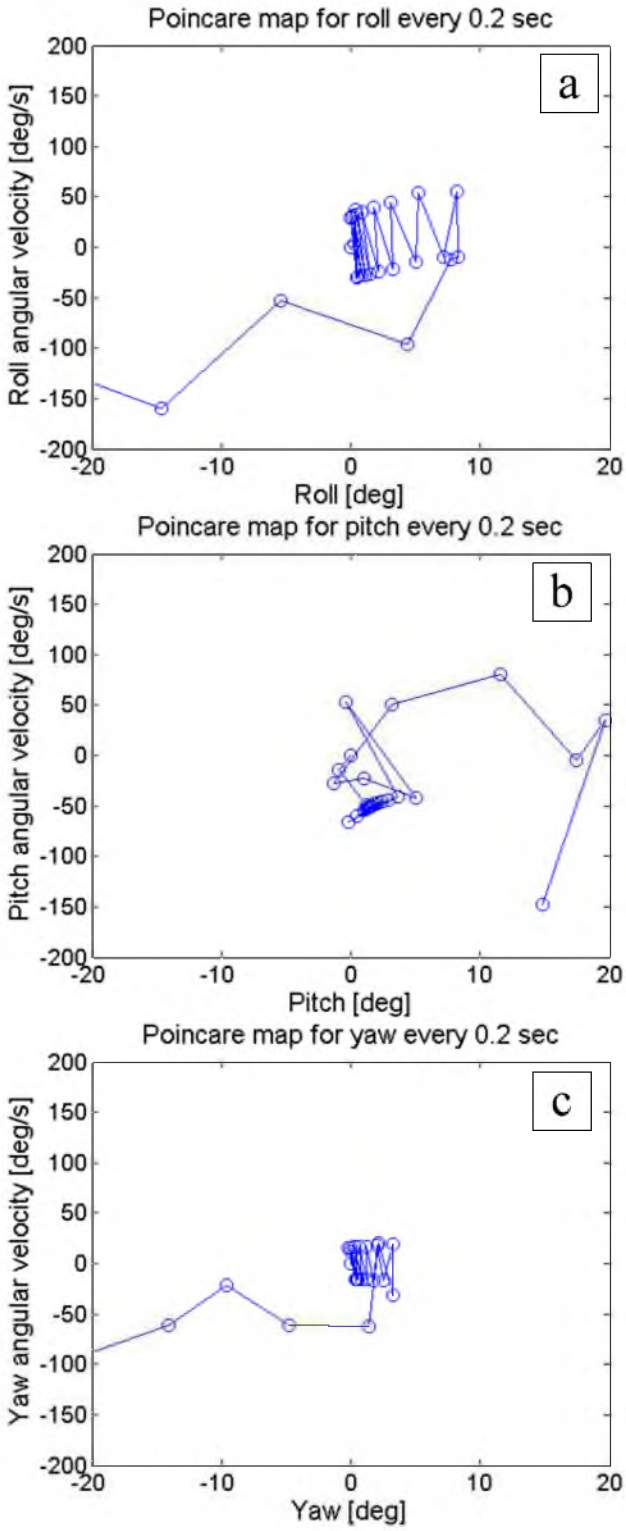

Fig. 18 - Poincaré maps of the backward leg configuration. (a) Roll angular velocity in terms of roll angle. (b) Pitch angular velocity in terms of pitch angle. (c) Yaw angular velocity in terms of yaw angle.

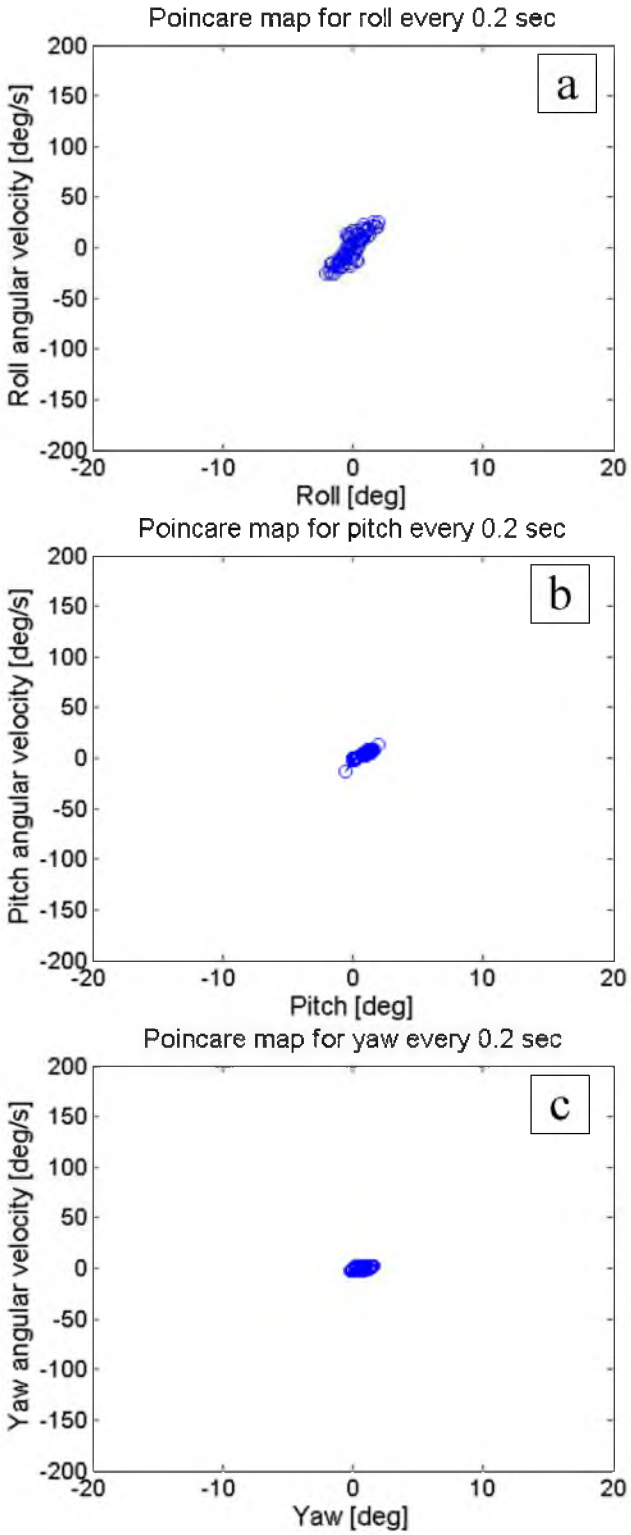

Fig. 19 - Poincaré maps of the forward leg configuration. (a) Roll angular velocity in terms of roll angle. (b) Pitch angular velocity in terms of pitch angle. (c) Yaw angular velocity in terms of yaw angle.

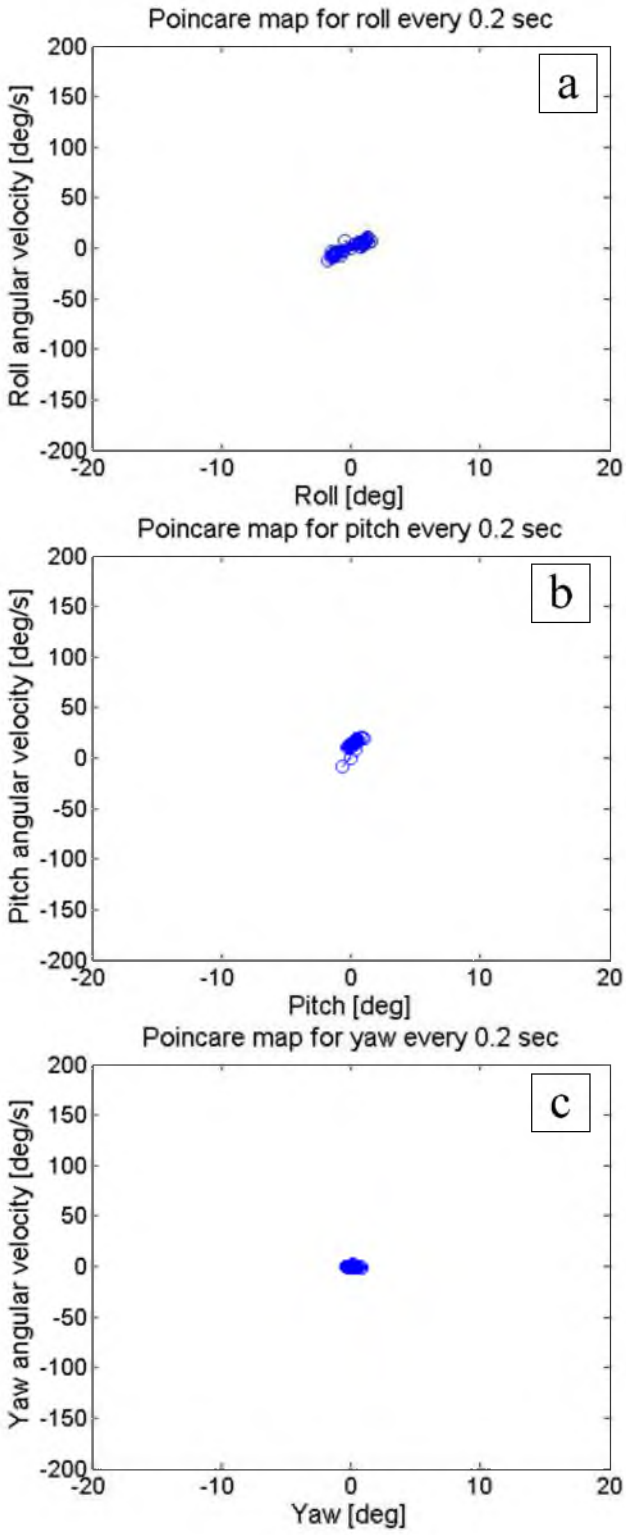

Fig. 20 - Poincaré maps of the natural leg configuration. (a) Roll angular velocity in terms of roll angle. (b) Pitch angular velocity in terms of pitch angle. (c) Yaw angular velocity in terms of yaw angle.

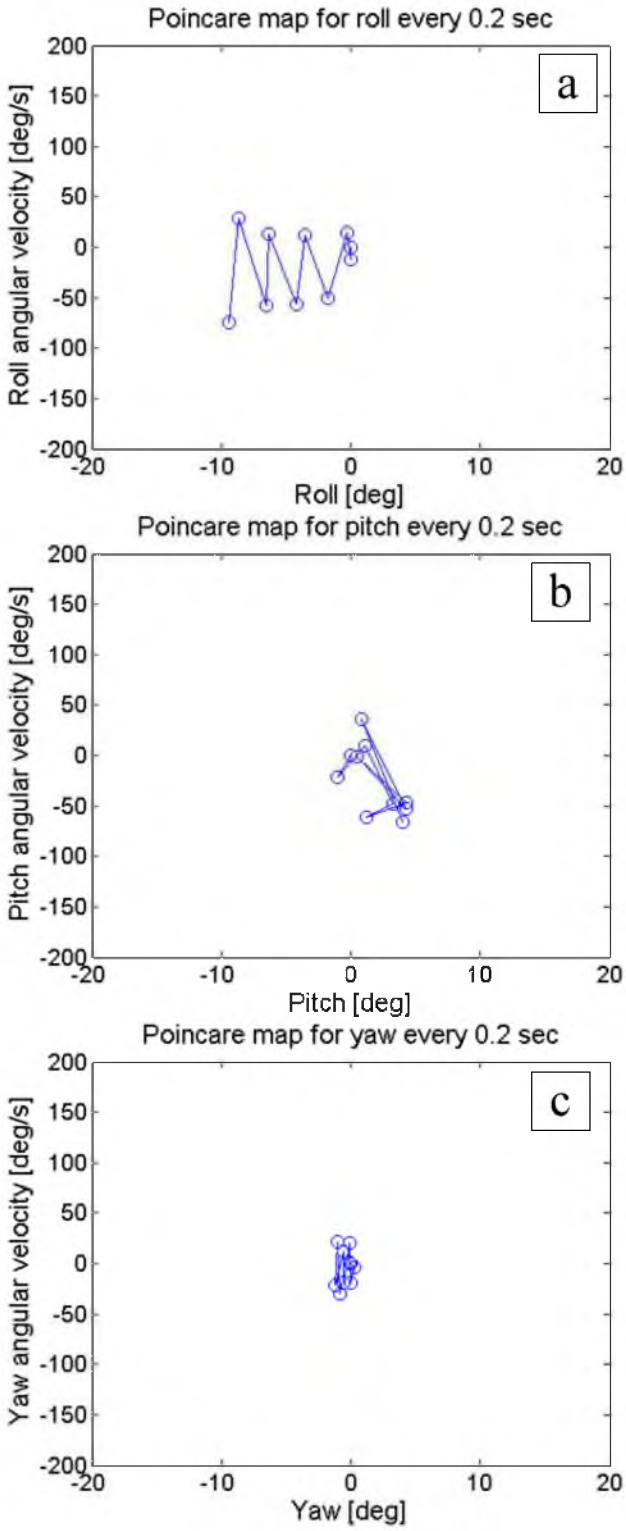

Fig. 21 - Poincaré maps of the reverse leg configuration. (a) Roll angular velocity in terms of roll angle. (b) Pitch angular velocity in terms of pitch angle. (c) Yaw angular velocity in terms of yaw angle.

Results presented in Fig. 22 show that the roll, pitch, and yaw fluctuations are minimum while the robot operates at Froude number of 1.2. They are also very small for a very fast trot. Froude number of 2.5 corresponds with average locomotion speed of 2.37 m/s, approximately eight body lengths per second. Using the same leg parameters for a slow trotting quadruped, resulted in a wobbly, yet, stable locomotion. The leg parameters may need to be tuned again for a slow trot gait.

Note that, Froude numbers are average because the speed and hip height changes trough the course of trotting.

Disturbance Rejection

In the transient and steady state analysis the ground was flat. However, real robots do not trot on flat ground. To get an understanding of the tolerance to disturbance, a set

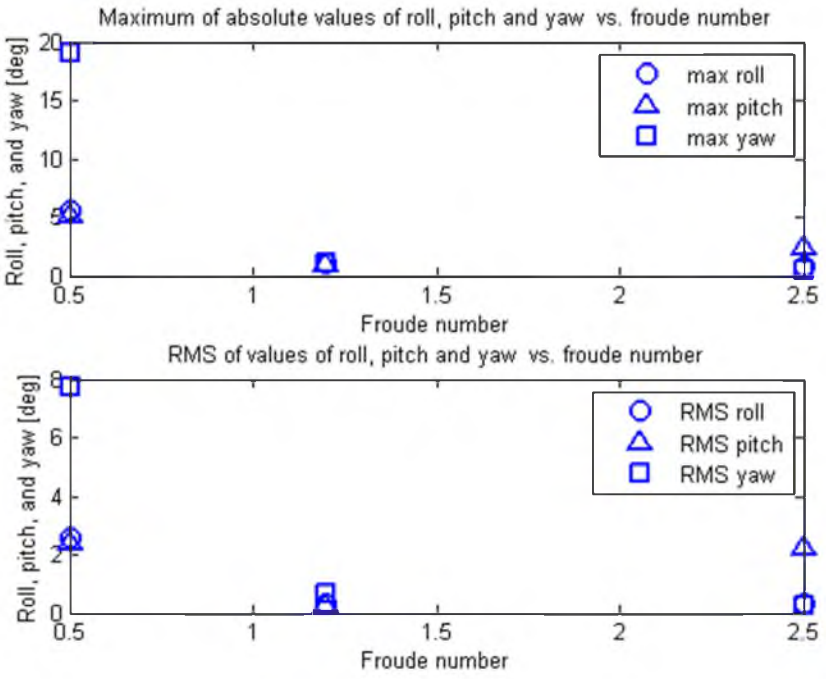

Fig. 22 - Maximum and RMS values of roll, pitch, and yaw for different speeds.

of simulations were performed to explore the effect of sudden changes in ground height on the overall stability of the robot. The disturbance was modeled as a hole in the ground. After 1 second (the transient phase is completely over) the robot's front left foot would step into a hole. The magnitude of the hole was set as a ratio of the robot's height to the depth of the hole. Simulations were performed using the optimum values that were found for every parameter in the previous section. Results exposed that the robot is not capable of passively maintaining balance under the influence of disturbances greater than 2% of the robot's height (Fig. 23). Afterwards, the disturbance was modeled as a step. Using the optimal leg parameters found in previous section, the robot showed ability to passively maintain balance for steps with a height of 2% of the robot's height (Fig. 24). Although; sharp peaks were detected throughout the simulation (mainly, right after the first second of the simulation which is the time when the disturbance was applied), the robot motion stabilized after a short while.

Results illustrated in Figs. 23 and 24 indicate that the primary mode of instability when the quadruped encounters a disturbance is usually due to the pitch behavior of the robot. This is expected, because when the robot's front leg strides into a hole or on a step, a severe change in the pitch occurs, which is sometimes impossible for the robot to recover from.

Finally, the knee/elbow stiffness, ankle/wrist stiffness and attenuation rates were varied simultaneously to study the effects of these parameters on disturbance rejection. The goal was to find a set of leg parameters for a trotting quadruped robot that can maintain balance after encountering a hole with a depth of 5% of the robot's height. It was desired to investigate if the robot leg stiffness needs to be tuned again, or the

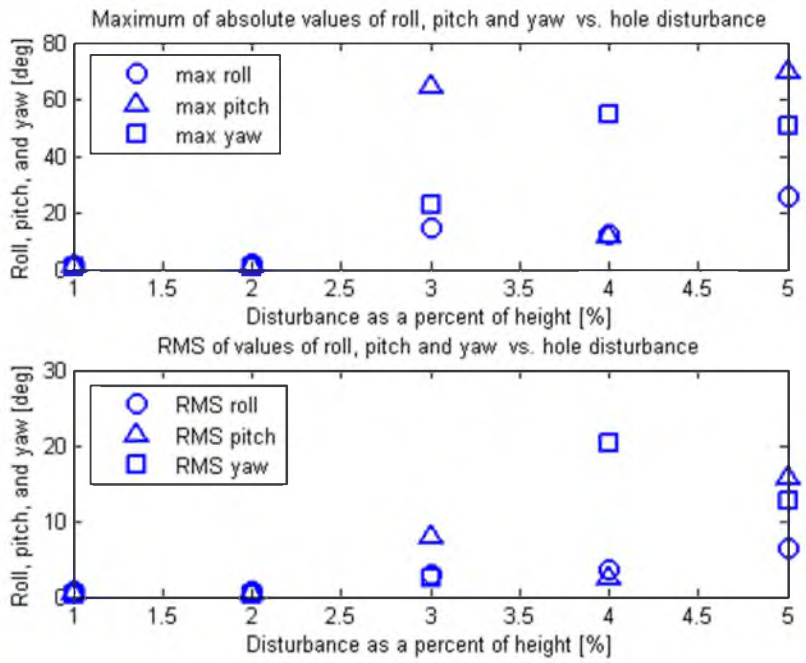

Fig. 23 - Maximum and RMS values of roll, pitch, and yaw for the trotting robot encountering a hole disturbance.

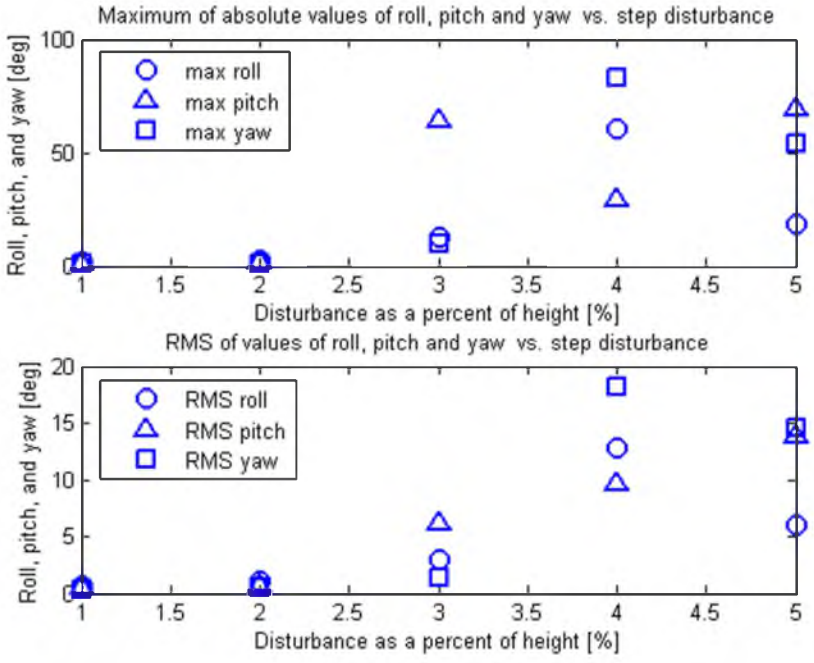

Fig. 24 - Maximum and RMS values of roll, pitch, and yaw for the trotting robot encountering a step disturbance.

previous results are also optimal for disturbance rejection. One hundred simulations were performed varying knee/elbow stiffness in the range of 0.1-10 (N m/deg), and ankle/wrist stiffness was varied from 1 to 10 (kN/m).

Results show that (Fig. 25-30), the previous optimal parameters from steady-state analysis, do not minimize the roll, pitch, and yaw behavior of the robot and they have to be tuned again. Ankle/Wrist springs have to be modified to 1(kN/m). This is considered as a soft spring and it did not have the best performance in steady state analysis. However, it appears to have the best performance for the purpose of disturbance rejection. In general it is advised that fairly stiff springs should be augmented in the lower distal leg and utilizing moderately soft springs for the upper distal leg would result in the best disturbance rejection results.

Secondly simulations indicate that robot's roll behavior is in contrast with its pitch attitude. This designates to two different falling behaviors. One is rotating over from the top which would result in increase of pitch. The other one is falling from the side, which would increase the roll angle of the quadruped robot.

The primary mode of failure (instability) for a trotting robot suffering from such disturbances would be due to high pitches and falling over from the top. This was expected, because a high speed trotting quadruped suddenly stepping leg into a hole with its front leg would most likely tend to pitch and rotate about the front leg.

Simulations suggest that only a robot utilizing fairly soft springs at lower distal leg is capable of overcoming high disturbances. In order to make sure the results are valid, and to explore the stable range more thoroughly, 100 more simulations were performed varying knee/elbow stiffness in the range of 0.1-1 (N m/deg), and ankle/wrist stiffness between 500-1400 (N/m). Results are illustrated in Fig. 31-36.

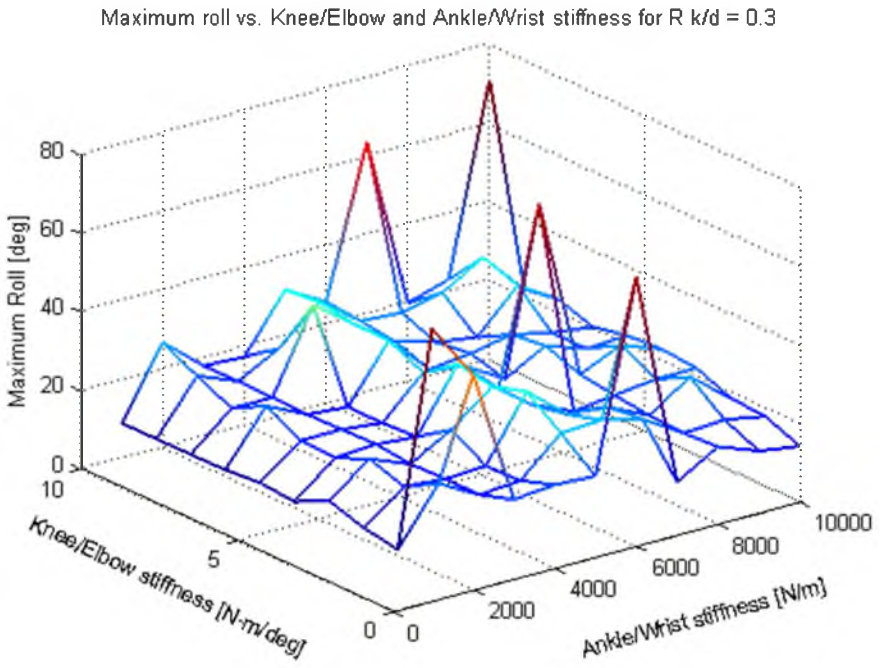

Fig. 25 - The effect of knee/elbow stiffness and ankle/wrist stiffness on the maximum of absolute of roll for the model encountering a disturbance. Knee/elbow stiffness was varied in the range of 0.1-10 (N m/deg), and ankle/wrist stiffness was varied in the range of 1-10 (kN/m).

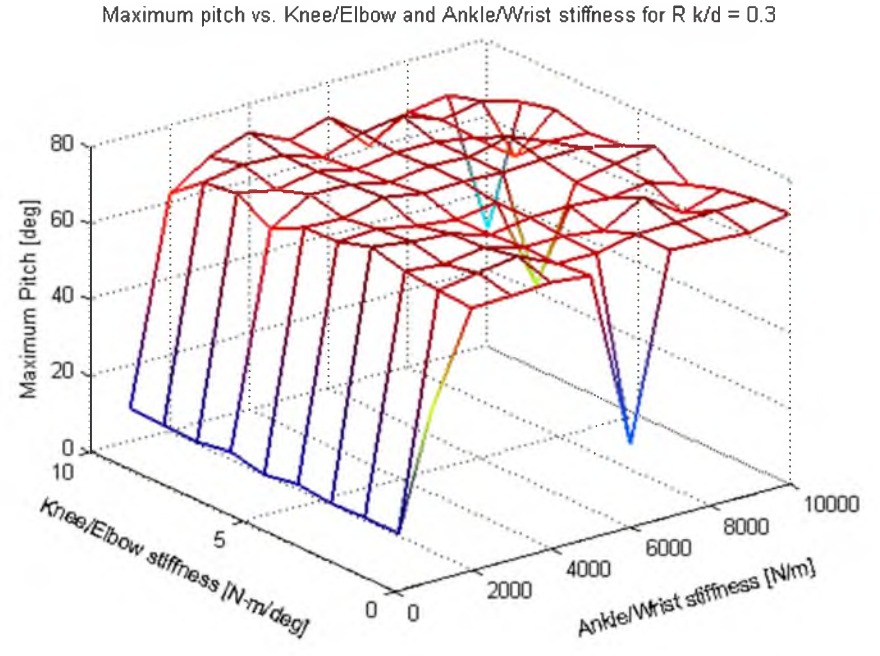

Fig. 26 - The effect of knee/elbow stiffness and ankle/wrist stiffness on the maximum of absolute of pitch for the model encountering a disturbance.

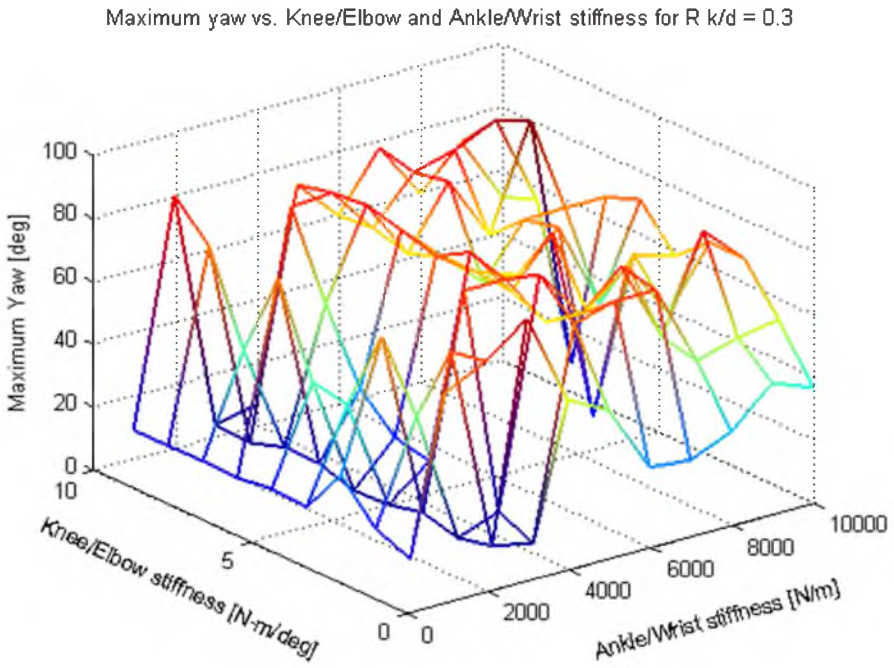

Fig. 27 - The effect of knee/elbow stiffness and ankle/wrist stiffness on the maximum of absolute of yaw for the model encountering a disturbance.

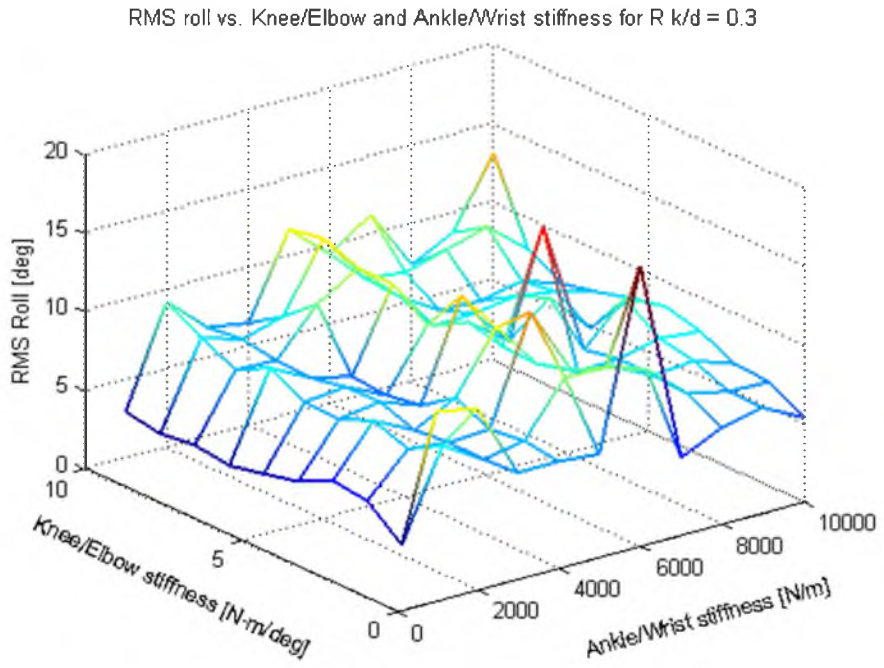

Fig. 28 - The effect of knee/elbow stiffness and ankle/wrist stiffness on the RMS of values of roll for the model encountering a disturbance.

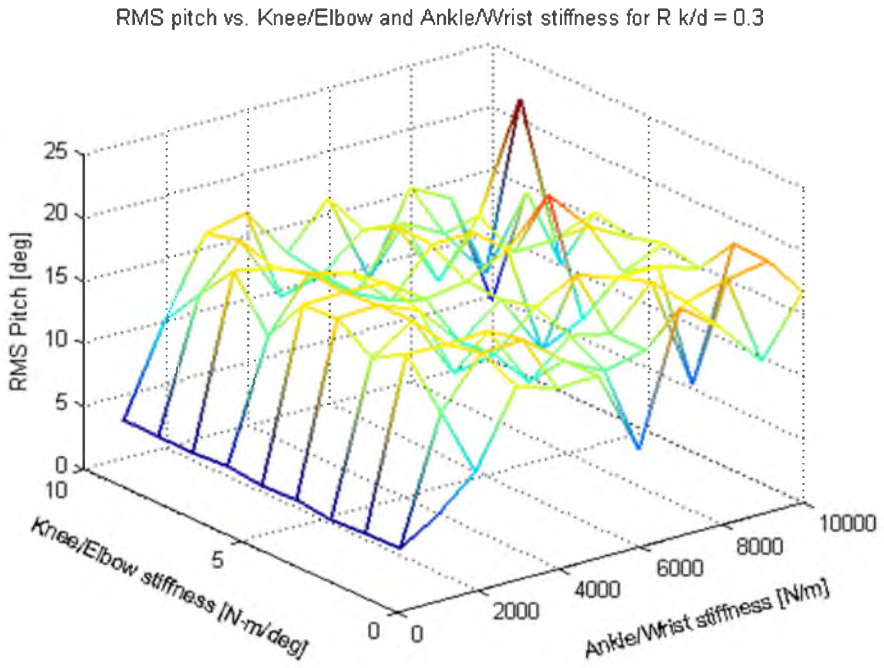

Fig. 29 - The effect of knee/elbow stiffness and ankle/wrist stiffness on the RMS of values of pitch for the model encountering a disturbance.

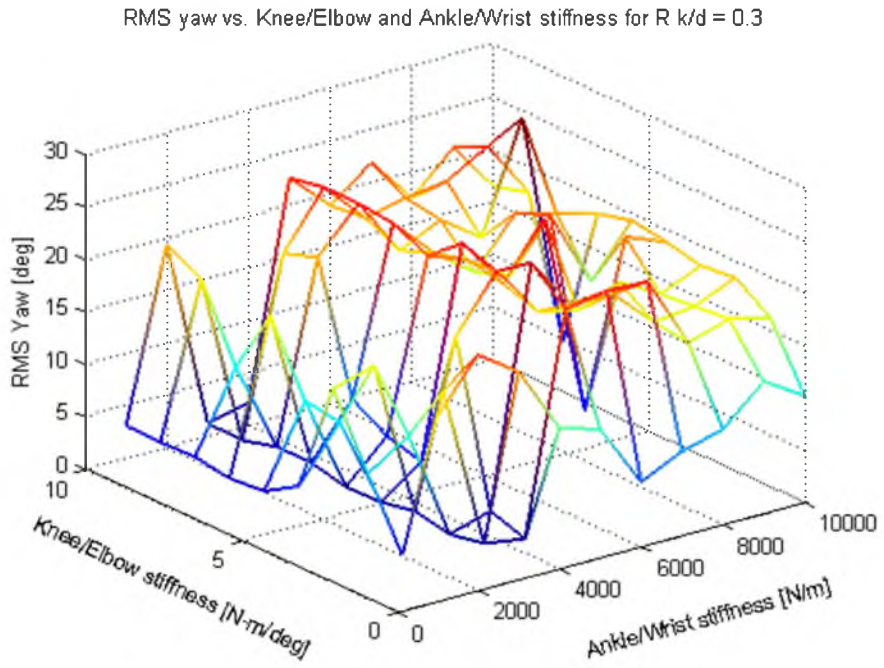

Fig. 30 - The effect of knee/elbow stiffness and ankle/wrist stiffness on the RMS of values of yaw for the model encountering a disturbance.

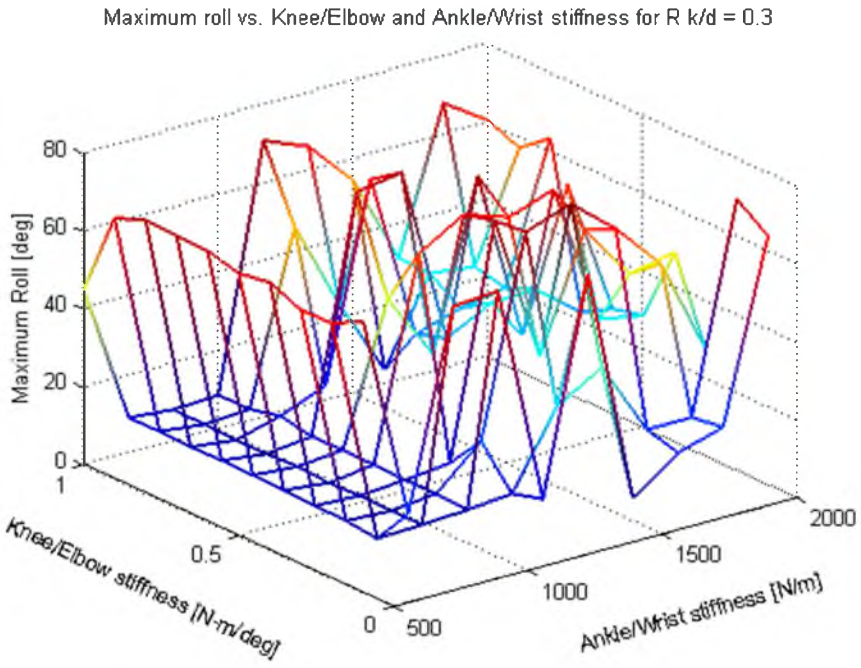

Fig. 31 - The effect of knee/elbow stiffness and ankle/wrist stiffness on the maximum of absolute of roll for the model encountering a disturbance. Knee/elbow stiffness was varied in the range of 0.1-1 (N m/deg), and ankle/wrist stiffness was varied in the range of 500-1400 (N/m).

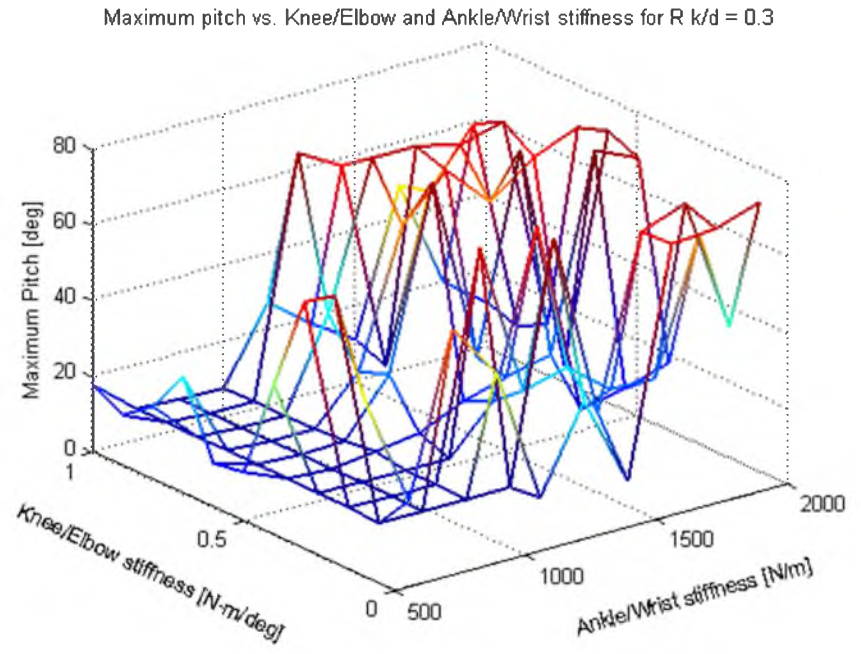

Fig. 32 - The effect of knee/elbow stiffness and ankle/wrist stiffness on the maximum of absolute of pitch for the model encountering a disturbance.

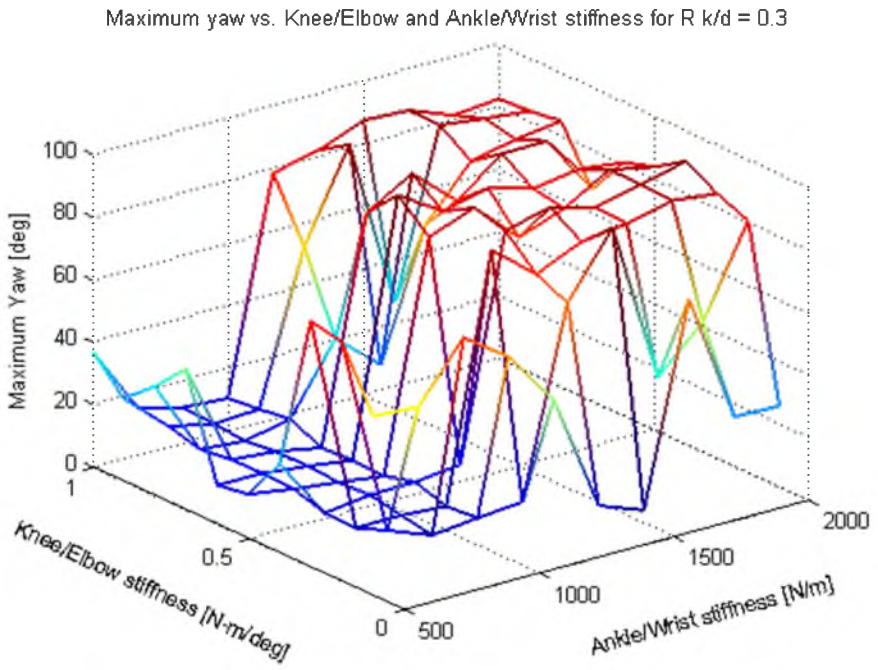

Fig. 33 - The effect of knee/elbow stiffness and ankle/wrist stiffness on the maximum of absolute of yaw for the model encountering a disturbance.

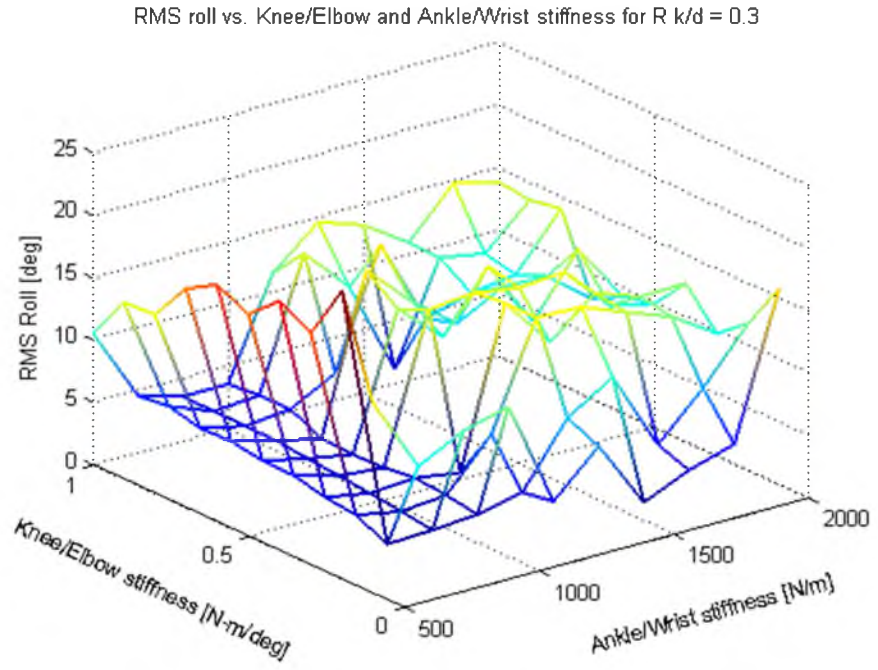

Fig. 34 - The effect of knee/elbow stiffness and ankle/wrist stiffness on the RMS of values of roll for the model encountering a disturbance.

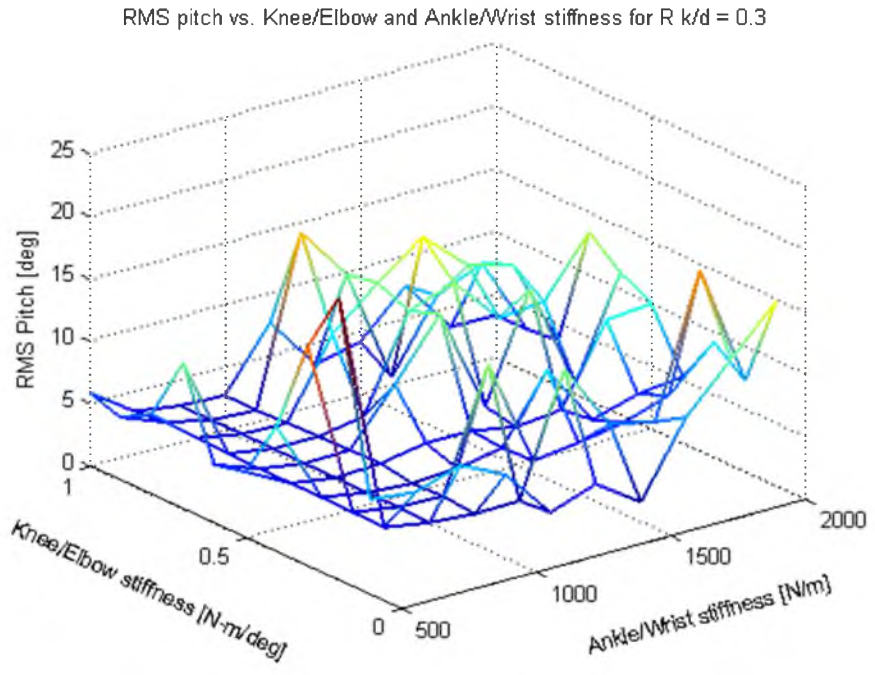

Fig. 35 - The effect of knee/elbow stiffness and ankle/wrist stiffness on the RMS of values of pitch for the model encountering a disturbance.

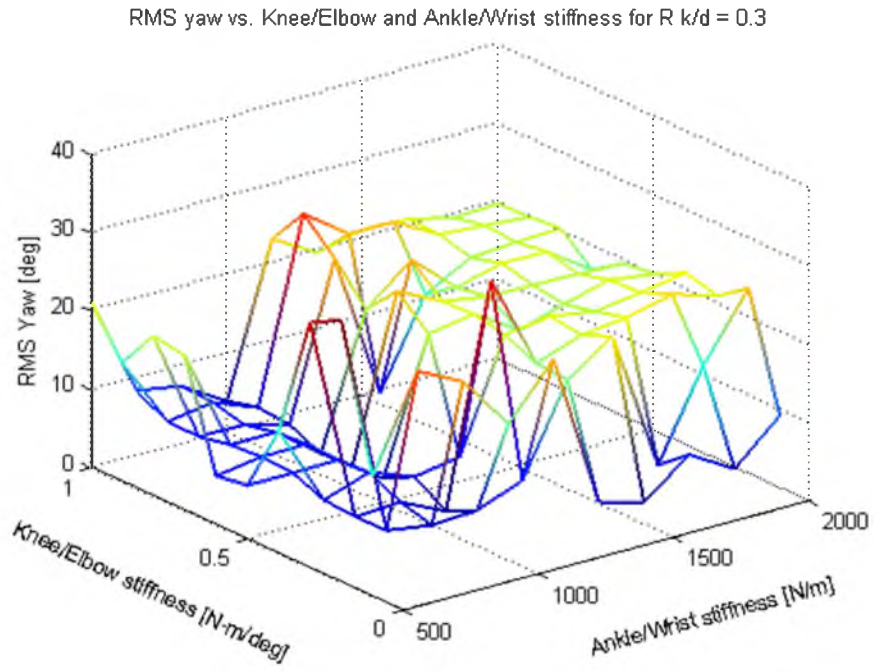

Fig. 36 - The effect of knee/elbow stiffness and ankle/wrist stiffness on the RMS of values of yaw for the model encountering a disturbance.

More simulations were performed to find the highest disturbance that the robot could tolerate and keep on moving on a stable attitude. Results confirmed that the highest disturbance that the robot could endure through the course of trotting was 6% percent of the robots height (Fig. 37). The robot cannot passively damp higher disturbances and other strategies such as active control paradigm should be employed. Optimal parameters for the purpose of disturbance rejection are presented in Table 3.

Discussion

Motor Torques

Reaction torque measured at the shoulder joint of the right fore leg is shown in Fig. 38. This is the same as the motor torque needed to actuate the legs. A quick

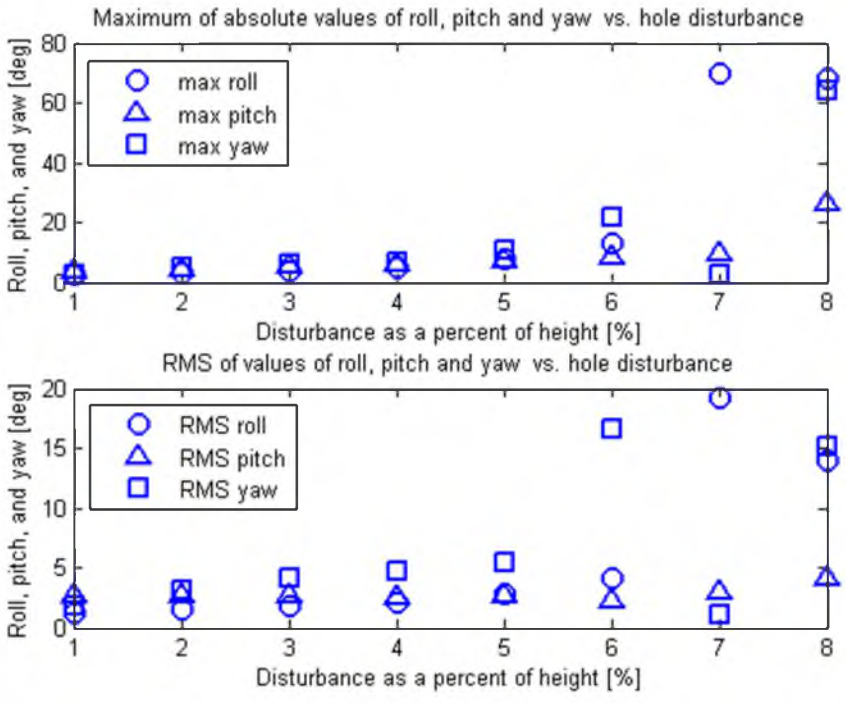

Fig. 37 - Maximum and RMS values of roll, pitch, and yaw for the trotting robot encountering a hole disturbance. The robot cannot endure disturbances higher than 6% of the robot's height.

Table 3. List of parameters, their ranges and optimal values for disturbance analysis

Variable Name	Symbol	Range	Optimal Value
Hip/Shoulder Stiffness	k_{hs}	10 (kN-m/deg)*	10 (kN-m/deg)
Alpha	α	-13°*	-13°
Knee/Elbow Stiffness	K_{ke}	0.1-10 (kN-m/deg)	0.5 (kN-m/deg)
Ankle/Wrist Stiffness	K_{aw}	1–10 (kN /m)	1 (kN /m)
Attenuation Rate	$R_{k/d}$	0.1, 0.3, 0.5 (s)	0.3 (s)
Stride Length		30° (±15°)*	30° (±15°)
Hind to Fore Leg Ratio		1*	1
Theta	θ	20°*	20°

*Previous (steady-state) optimal parameter was used in this study

calculation showed that the torque is realistic and the commercial motors are capable of producing such torques.

Note that a full stride cycle occurs in 0.2 seconds, and the right front leg is initially at the end of stance phase and the beginning of flight phase. Positive peaks occur a moment after the foot touches the ground (beginning of stance phase). The reason is the thrust forces needed to carry the body forward is generated by propulsive torques at the shoulders. Negative peaks occur at the end of stance phase when the robot is bringing the leg to the start of flight phase.

Comparison of Steady-state and Disturbance Optimal Parameters

Two sets of optimal parameters are found and were presented in Tables 2 and 3. Using the steady-state optimal parameters on a quadruped that trots on a flat ground, results in minimum roll, pitch, and yaw motion. The maximum of roll, pitch, and yaw are about 1 degree and the RMSs are very small. Using these parameters under the influence of disturbances, the quadruped can only take disturbances as high as 2% of the body's height.

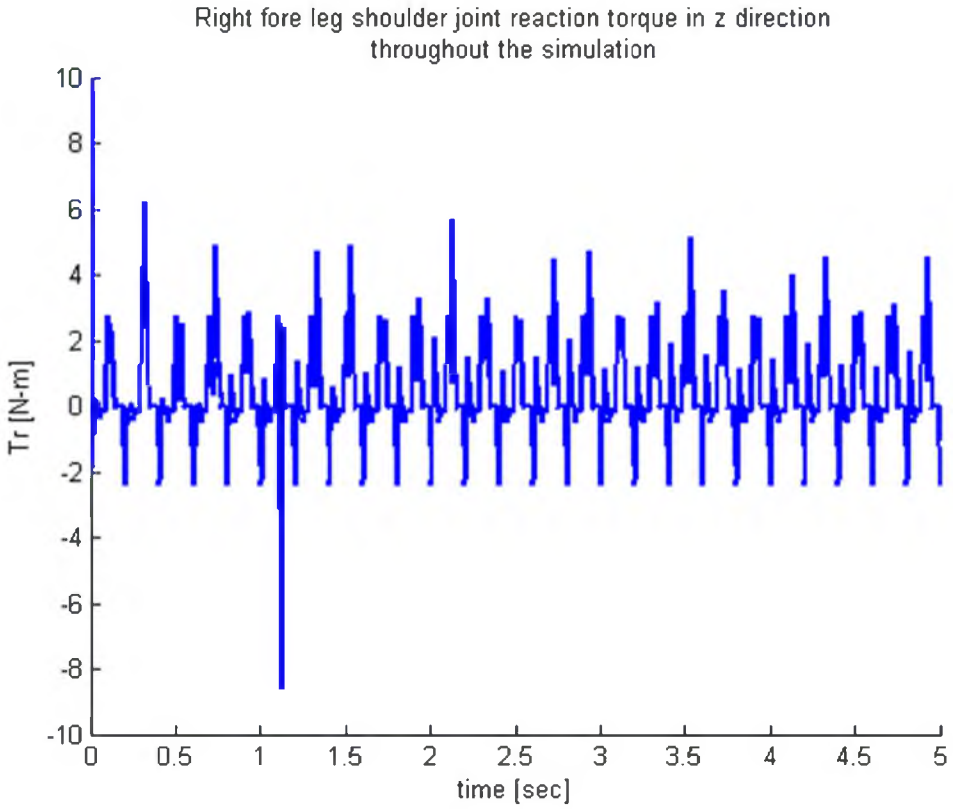

Fig. 38 – Reaction torque in z direction exerted to the right fore leg's shoulder joint.

Optimal parameters tuned for disturbance rejection, result in stable trot on flat ground with maximum roll, pitch, and yaw of about 4 degrees. However, the robot can maintain balance after imposing disturbances up to 5% of the body's height. It is good to mention that 5% disturbance results take larger values than flat ground results. This was expected because a huge disturbance was present in that experiment. Comparison of the results is presented in Table 4.

Variations of roll, pitch, and yaw throughout four diverse simulations are illustrated in Fig. 39 – 42. The disturbance is imposed to the trotting quadruped at time equal to 1.2 sec. Figures 40 and 42 show that a dramatic change in robot's roll and pitch occur after stepping into a hole.

Table 4. Comparison of steady-state and disturbance optimal parameters

	Flat Ground Simulation			Under Disturbance		
	Max Roll* (RMS)	Max Pitch (RMS)	Max Yaw (RMS)	Max Roll (RMS)	Max Pitch (RMS)	Max Yaw (RMS)
Steady-state Parameters	1.10 (0.33)	0.99 (0.24)	1.10 (0.66)	Only up to 2%	Only up to 2%	Only up to 2%
Disturbance Parameters	3.72 (1.53)	4.68 (2.94)	4.04 (2.48)	7.74 (2.79)	7.39 (2.61)	10.44 (5.49)

*All values are in degrees

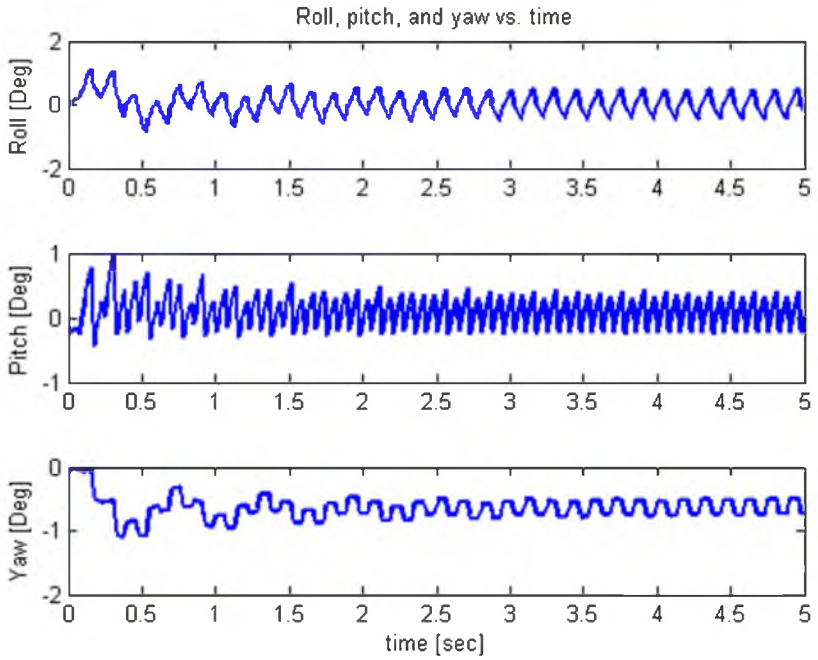

Fig. 39 – Variations in roll, pitch, and yaw throughout a steady-state simulation, using flat ground optimal leg parameters.

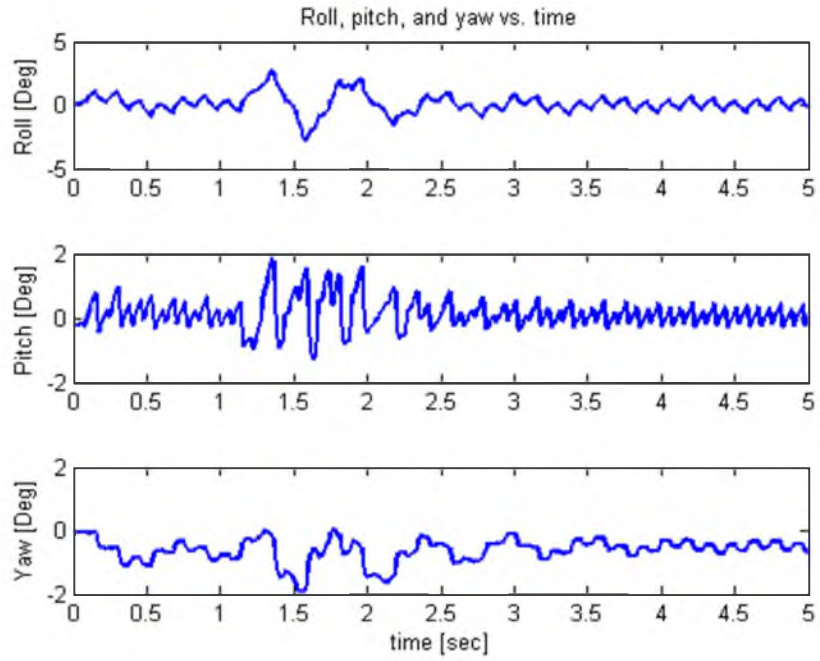

Fig. 40 - Variations in roll, pitch, and yaw throughout a simulation with 2% disturbance, using flat ground optimal leg parameters. Disturbance is imposed to the quadruped at time equal to 1.2 sec.

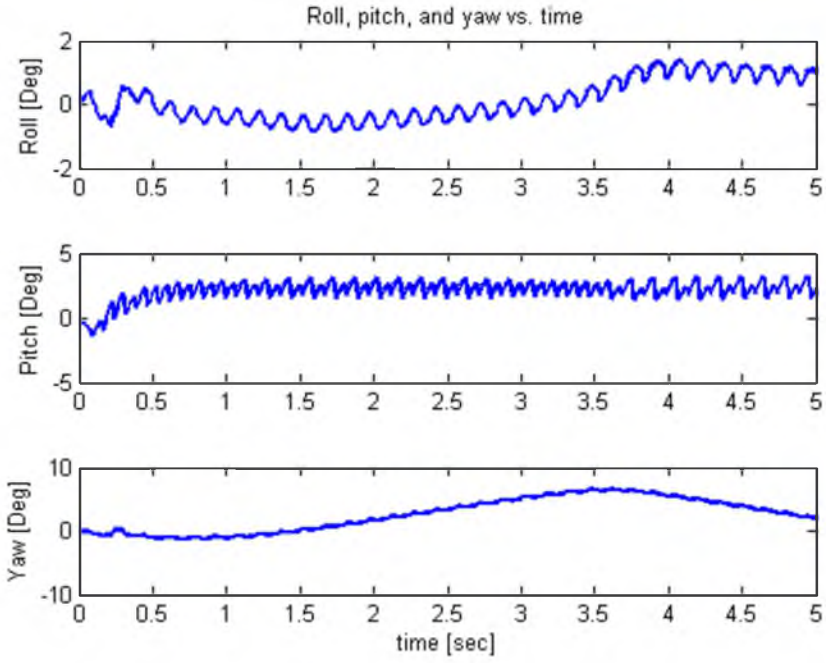

Fig. 41 – Variations in roll, pitch, and yaw throughout a steady-state simulation, using disturbance optimal leg parameters.

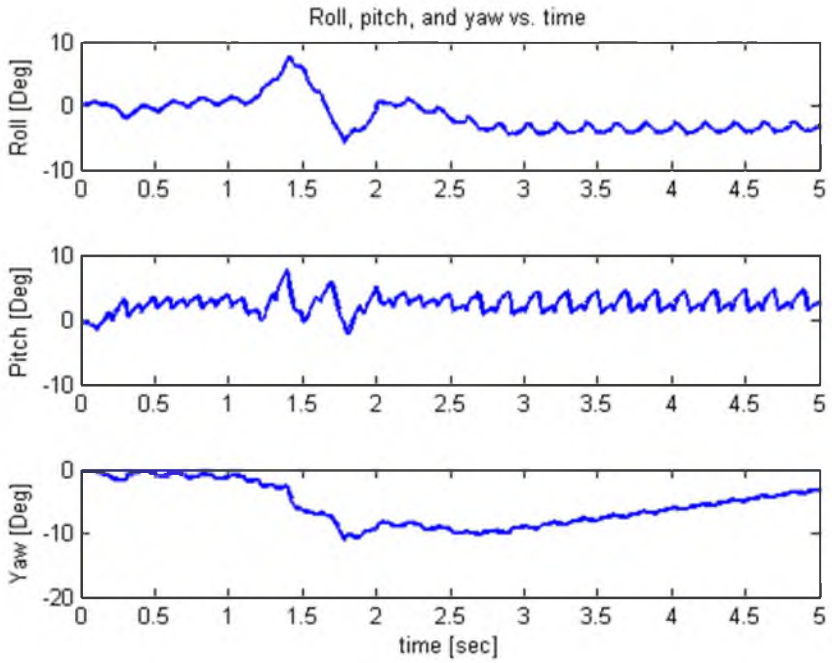

Fig. 42 - Variations in roll, pitch, and yaw throughout a simulation with 5% disturbance, using flat ground optimal leg parameters. Disturbance is imposed to the quadruped at time equal to 1.2 sec.

Nondimensional Analysis

Heglund and Taylor [45] studied different species of animals and provided the following equations that relate the animal's body mass to its trotting speed:

$$minimum\ trotting\ speed = 0.593\ M_b^{0.249} \tag{4.1}$$

$$preferred\ trotting\ speed = 1.09\ M_b^{0.22} \tag{4.2}$$

$$trot - gallop\ transition\ speed = 1.54\ M_b^{0.216} \tag{4.3}$$

where M_b is the animal's body mass. For our 5.7 kg quadruped, these speeds are approximately 0.91, 1.6, and 2.24 m/s respectively. In simulations, minimum trotting speed, optimal trotting speed and maximum trotting speed were 1.08, 1.73, and 2.37 m/s, respectively.

CHAPTER 5

CONCLUSIONS AND FUTURE WORK

The primary goal of this research was to determine means of stabilizing a trotting quadruped model by determining the optimal leg configurations. To that end, a detailed analysis has been presented that examines the effect of different parameters on stability. Ultimately, a steady-state and a disturbance response were utilized to achieve the best leg configuration. The simulations demonstrate that by operating stiff springs at hips and shoulders, soft spring at knees and elbows, and stiff springs at ankles and wrists, not only passive stability of a trotting quadruped is achievable, but also the fluctuations in the roll, pitch, and yaw are minimal.

Finally, the disturbance responses were observed in a situation where the robot steps into a hole with one of its front legs. The pitching and rolling results indicated that in order to best respond to a disturbance in ground height, a soft torsional spring for the knee/elbow joint and rather stiff springs for the ankle/wrist joints should be augmented. Very stiff shoulder and hip springs are always advised.

The results of this project provide a conceptual framework for understanding the movements of a trotting quadruped. In this work we present a quadruped model that requires only two motors to navigate. Thus, it is much more energy efficient. Velocity

profiles are provided to the motors to match the characteristics of the trot gait and desired speed.

Researchers [42-44]; were able to achieve trotting speeds as high as 5.25 m/s, approximately four body lengths per second, by utilizing a very complex control algorithm. By passively actuating the legs due to desired velocity profiles, and utilizing appropriate leg stiffness, we were able to achieve maximum stable trotting speeds of 2.37 m/s, approximately eight body lengths per second. No feed-back or feed-forward control algorithm was used on this experiment.

Palmer's robot was able to maneuver over uneven terrain with standard deviation of height variation of 3 cm at 4.0 m/s (maximum terrain elevation of 6.5 cm, which was greater than 10% of the nominal leg length). However, he used panels to model the uneven terrain. Each floor panel was 60 cm in length (almost half of the robot's length). The elevation of each panel was randomly selected from a normal distribution, resulting in a highly smooth change in elevation.

Our trotting robot model was able to overcome disturbances in the form of step and hole with the height and depth of 6% of the body's height, respectively. The disturbance was applied to the robot after a few full stride cycles. The robot's right fore leg stepped into a hole (stepped on a stair) while trotting at 1.73 m/s, approximately six body lengths per second. The robot showed less capacity to overcome disturbances, compared to Palmer's robot, but it should be noted that no control algorithm was used to return the robot to balance and the robot was able to maintain balance passively.

This appears to be the first 3D analysis of a trotting quadruped robot that utilizes passive under-actuated compliant legs. We showed that stable trotting is achievable

without using any control algorithm. Moreover, the robot is able to passively maintain balance after encountering disturbances.

Future Work

A reality-based simulation frame work that is not confined to sagittal plane motion was presented in this project. The main purpose of this project was to determine the passive stability of a trotting quadruped in 3D utilizing complaint under-actuated legs. Means to optimize the roll, pitch, and yaw behavior of the robot was presented. As the design space is large, simulations rather than analytical solution was pursued. Brute force was employed to search the design space. However, it is recommended to use a direct search optimization such as Nelder-Mead Simplex Method or possibly a genetic algorithm.

This basic conceptual framework could be used to explore the behavior of a large variety of animals by simply editing the dimensions and mass properties of the main body and legs. Moreover, numerous gaits could be simulated and analyzed since this research was only confined to a trotting gait. Last but not least, the quadruped behavior during gait transition could be analyzed, since there has been only a limited researched done on this topic.

REFERENCES

[1] M. H. Raibert, "Trotting, pacing and bounding by a quadruped robot," Journal of Biomechanics, vol. 23, pp. 79-98, 1990

[2] T. McGeer, "Passive bipedal running," Technical Report CCS-IS TR , Simon Fraser University.

[3] T. McGeer, "Passive dynamic walking," The International Journal of Robotics Research, vol. 9, no. 2, pp. 62-82, 1990

[4] S.P.N Singh, K.J. Waldron, "Attitude estimation for dynamic legged locomotion using range and inertial sensors," The IEEE of International Conference on Robotics and Automation (ICRA), Barcelona, Spain, pp. 1663 – 1668, 2005

[5] M.D. Berkemeier, "Self-organizing running in a quadruped robot model," The IEEE of International Conference on Robotics and Automation (ICRA), Barcelona, Spain, pp. 4108 – 4113, 2005

[6] S.P.N Singh, K.J. Waldron, "System design of a quadrupedal galloping machine," The International Journal of Robotics Research, vol. 23, no. 10-11, pp. 1013-1027, 2004

[7] H. Herr, T. McMahon, "A trotting horse model," The International Journal of Robotics Research, vol. 19, no. 6, pp. 566-581, 2000

[8] H. Herr, T. McMahon, "A galloping horse model," The International Journal of Robotics Research, vol. 20, no. 1, pp. 26-37, 2001

[9] M.D. Berkemeier, "Modeling the dynamics of quadrupedal running," The International Journal of Robotics Research, vol. 17, no. 9, 971-985, 1998

[10] G. Hawker, M. Buehler, "Quadruped trotting with passive knees – design, control, and experiments," The IEEE of International Conference on Robotics and Automation (ICRA), San Francisco, USA, vol. 3, pp. 3046 - 3051, 2000

[11] D. Lee, S. Meek, "Directionally compliant legs influence the intrinsic pitch behavior of a trotting quadruped," Proceedings of the Royal Society B: Biological Sciences, vol. 272, no. 1563, pp. 567-572, 2005

[12] M. de lasa, M. Buehler, "Dynamic compliant quadruped walking," The IEEE of International Conference on Robotics and Automation (ICRA), Seoul, Korea, vol. 3, pp. 3153 - 3158, 2001

[13] D. papadopoulus, M. Buehler, "Stable running in a quadruped robot with compliant legs," The IEEE of International Conference on Robotics and Automation (ICRA), San Francisco, USA, vol. 1, pp. 444 - 449, 2000

[14] M. Ahmadi, M. Buehler, "Stable control of a simulated one-legged running robot with hip and leg compliance," IEEE Trans. Robotics and automation, vol. 13, pp. 96 – 104, 1997

[15] I. Poulakakis, J. A. Smith, and M. Buehler, "Modeling and experiments of untethered quadrupedal running with a bounding gait: the scout II robot," The International Journal of Robotics Research, vol. 24, no. 4, pp. 239-256, 2005

[16] S. Meek, J. Kim, and M. Anderson, "Stability of a trotting quadruped robot with passive, under-actuated legs," The IEEE of International Conference on Robotics and Automation (ICRA), Pasadena, USA, pp. 347 - 351, 2008

[17] L. F. Shampine, M. W. Reichelt, "The MATLAB ODE Suite," Natick, MA: The MathWorks 1997

[18] G. D. Wood, D. C. Kennedy, "Simulating Mechanical Systems in Simulink with SimMechanics (91124v00)," Natick, MA: The Math Works 2003

[19] L. F. Shampine, Numerical Solution of Ordinary Differential Equations. CRC Press, 1994

[20] D. Lee, J. Bertram, and R. Todhunter, "Acceleration and balance in trotting dogs," Journal of Experimental Biology, 202, pp. 3565-3573, 1999

[21] M. Anderson, "Design of a trotting quadruped robot," M.S. thesis, Dept. Mech. Eng., Univ. of Utah, Salt Lake City, Utah, 2004.

[22] R. McNeil Alexander, Principles of Animal Locomotion. Princeton University Press, 2003

[23] G. C. Haynes, A. A. Rizzi, "Gaits and gait transitions for legged robots," The IEEE of International Conference on Robotics and Automation (ICRA), Orlando, USA, pp. 1117 - 1122, 2006

[24] J. Schmiedler, K. Waldron, "The significance of leg mass in modeling quadruped running gaits," to appear in proceedings of CISM/FToMM symposium on robots and manipulators, Udine, Italy July 1-4, 2002

[25] T. A. McMahon "The role of compliance in mammalian running gaits," Journal of Experimental Biology, 115, pp. 263-282, 1985

[26] T. A. McMahon, G. Cheng "The mechanics of running: how does stiffness couple with speed," Journal of Experimental Biology, 23, pp. 65-78, 1990

[27] M. H. Raibert, Legged Robots that Balance. Cambridge, Mass: MIT Press. 1986

[28] J. Gray, Animal Locomotion. New York: Norton, 1986

[29] C. D. Remy, K. Buffinton, and R. Siegwart, "Stability analysis of passive dynamic walking of quadrupeds," The International Journal of Robotics Research, vol. 29, no. 9, pp. 1173-1185, 2010

[30] M. H. Raibert, "Legged robots," Communications of the ACM, vol. 29, no. 6, pp. 499 - 514, 1986

[31] G. A. Pratt, and M. M. Williamson, "Series elastic actuators," The International Conference on Intelligent Robots and Systems (IEEE/RSJ), vol. 1, pp. 399 - 406, 1995

[32] D. P. Krasny, D. E. Orin, "Generating high-speed dynamic running gaits in a quadruped robot using an evolutionary search," IEEE Trans. Systems, Man, and Cybernetics, Part B: Cybernetics, vol. 34, pp. 1685 - 1696, 2004

[33] D. W. Marhefka, D. E. Orin, J. P. Schmiedeler, K. J. Waldron, "Intelligent control of quadruped gallops," IEEE/ASME Trans. on Mechatronics, vol. 8, pp. 446 - 456, 2003

[34] J. G. Nichol, S. P.N. Singh, K. J.Waldron, L. R. Palmer III, D. E. Orin, "System Design of a Quadrupedal Galloping Machine," The International Journal of Robotics Research, vol. 23, no. 10-11, pp. 1013-1027, 2004

[35] H. E. Susan, Horse Gaits, Balance, and Movements. Howell Book House, 1993

[36] C. Semini, N. G. Tsagarakis, E. Guglielmino, M. Focchi, F. Cannella, D. G. Caldwell, "Design of HyQ – a hydraulically and electrically actuated quadruped robot," The International Journal of Robotics Research, vol. 225, no. 6, pp. 831-849, 2011

[37] M. Laffranchi, N. G. Tsagarakis, D. G. Caldwell, "Analysis and development of a semiactive damper for compliant actuation systems," IEEE/ASME Trans. On Mechatronics, Issue. 99, pp. 1-10, 2012

[38] T. Boaventura, C. Semini, J. Buchli, and D. G. Caldwell, "Actively-compliant leg for dynamic locomotion," Int. Symp. Adaptive Motion of Animals and Machines (AMAM), 2011

[39] T. Boaventura, C. Semini, J. Buchli, M. Frigerio, M. Focchi, D.G. Caldwell, "Dynamic torque control of a hydraulic quadruped robot," The IEEE of International Conference on Robotics and Automation (ICRA), St. Paul, MN, USA, pp. 1889 - 1894, 2012

[40] D. F. Hoyt and C. R. Taylor, "Gait and the energetics of locomotion in horses," Nature, vol. 292, pp. 239–240, 1981.

[41] K. J. Waldron, and P. Nanua, "Energy comparison between trot, bound, and gallop using a simple model," Journal of Biomechanical Engineering, vol. 117, no. 4, pp. 466–473, 1995.

[42] L. R. Palmer III, and D. E. Orin, "Force redistribution in a quadruped running trot," The IEEE of International Conference on Robotics and Automation (ICRA), Rome, Italy, pp. 5743 – 5749, 2007

[43] L. R. Palmer III, and D. E. Orin, "Attitude control of a quadruped trot while turning," IEEE/RSJ International Conference on Intelligent Robots and Systems, pp. 5743 - 5749, 2006

[44] L.R. Palmer III, and D.E. Orin, "Quadrupedal running at high speed over uneven terrain," IEEE/RSJ International Conference on Intelligent Robots and Systems, pp. 303-308, 2007

[45] N. C. Heglund, and C. R. Taylor, "Speed, stride frequency and energy cost per stride: how do they change with body size and gait?" Journal of Experimental Biology, vol. 138, pp. 301–318, 1988

[46] M. H. Raibert, K. Blankespoor, G. Nelson, R. Playter, and the BigDog Team, "Bigdog the rough-terrain quadruped robot," In Proceedings of the 17th World Congress, The International Federation of Automatic Control (IFAC), 2008

[47] R. Playter, M. Buehler, and M. Raibert, "BigDog," Defense and Security Symposium, International Society for Optics and Photonics, 2006

[48] S. Nathan, "Marc Raibert of Boston dynamics," Source: Engineer, v 22-FEBRUAR, February 22, 2010

[49] M. Vukobratović, and B. Borovac. "Zero-moment point—thirty five years of its life," International Journal of Humanoid Robotics 1.01 (2004): 157-173